The Future Trends in Molecular Imaging

Dr. Juri Gelovani, MD, PhD.

Professor of
Radiology and Neurology

Chairman, Dept. Experimental Diagnostic Imaging

Director, Center for Advanced Biomedical Imaging Research (CABIR)

THE UNIVERSITY OF TEXAS
MD ANDERSON
CANCER CENTER
Making Cancer History™

Molecular And Genetic Imaging of Cancer

Early & Accurate Diagnosis

- To follow Biomarker Screening (blood genomics and proteomics)
- Develop Imaging of Biomarkers (tumor localization, sensitivity)

Tumor Phenotyping

- Tumor Profiling (receptors & signal transduction, invasiveness, metabolism, proliferation, apoptosis, etc.)
- Stroma Profiling (angiogenesis, tissue re-organization, etc.)

Imaging for Selection & Monitoring of Therapy

- Drug Target Expression & Activity
- Dose Optimization
- Early Response Evaluation (Rx adjustment)
- Short-term & Long Term Prognosis
- Monitoring Contained/Chronic Disease status
- Early Detection of Relapse

THE UNIVERSITY OF TEXAS MD ANDERSON CANCER CENTER
Making Cancer History™

Image-Guided Biopsy, Surgery and Radiotherapy

Image-Guided Biopsy

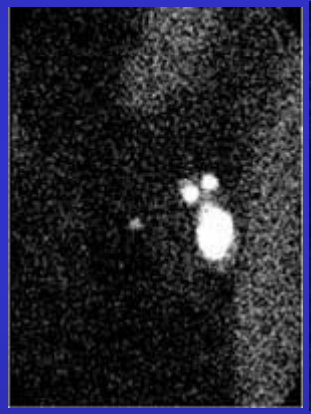

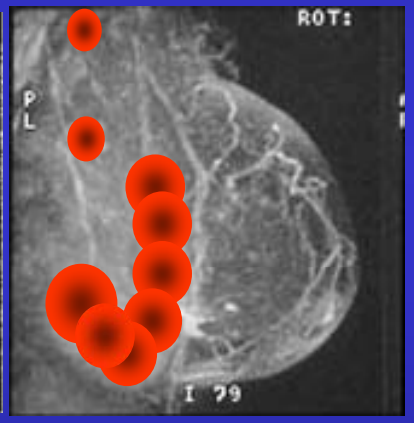

Image-Guided Radiotherapy

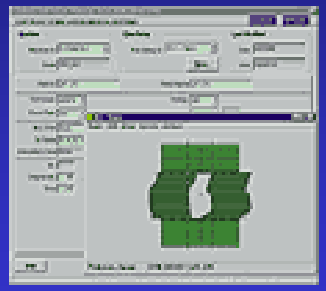

THE UNIVERSITY OF TEXAS
MD ANDERSON
CANCER CENTER
Making Cancer History™

Sentinel lymph node mapping in breast carcinoma patients

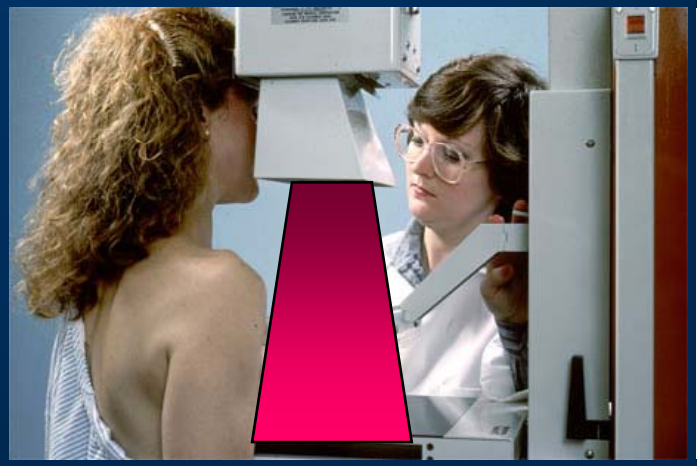

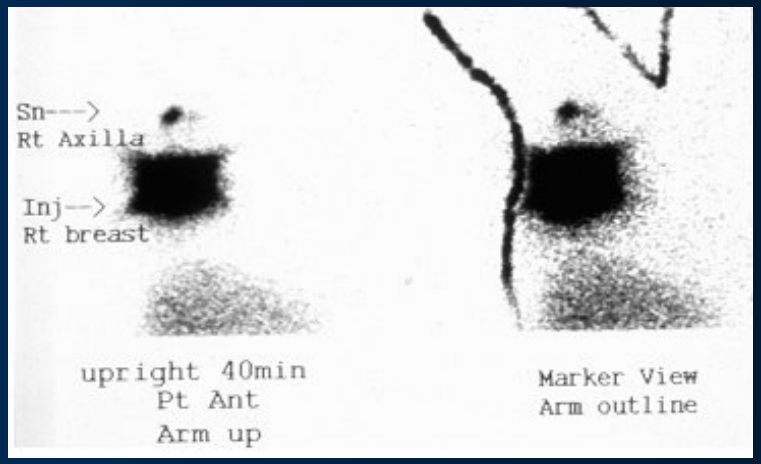

THE UNIVERSITY OF TEXAS
MD ANDERSON
CANCER CENTER
Making Cancer History™

Sentinel lymph node mapping in breast carcinoma patients

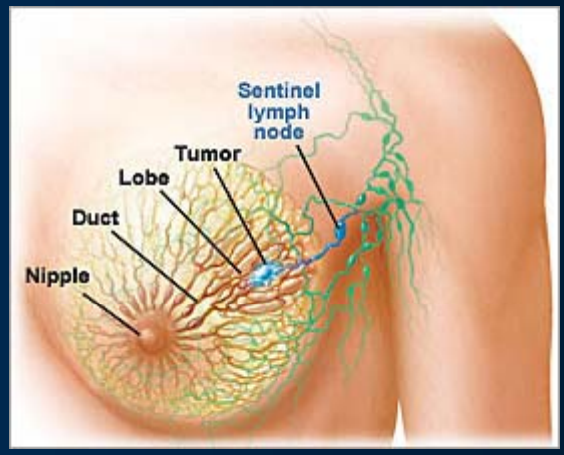

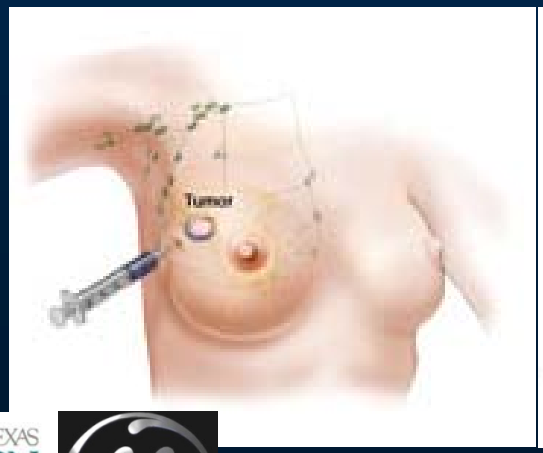

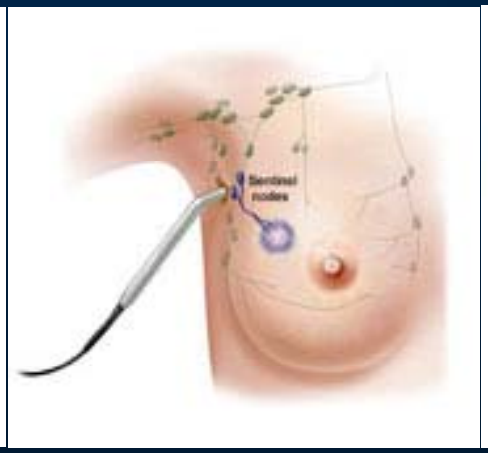

THE UNIVERSITY OF TEXAS
MD ANDERSON
CANCER CENTER
Making Cancer History™

Imaging of angiogenesis in breast tumor

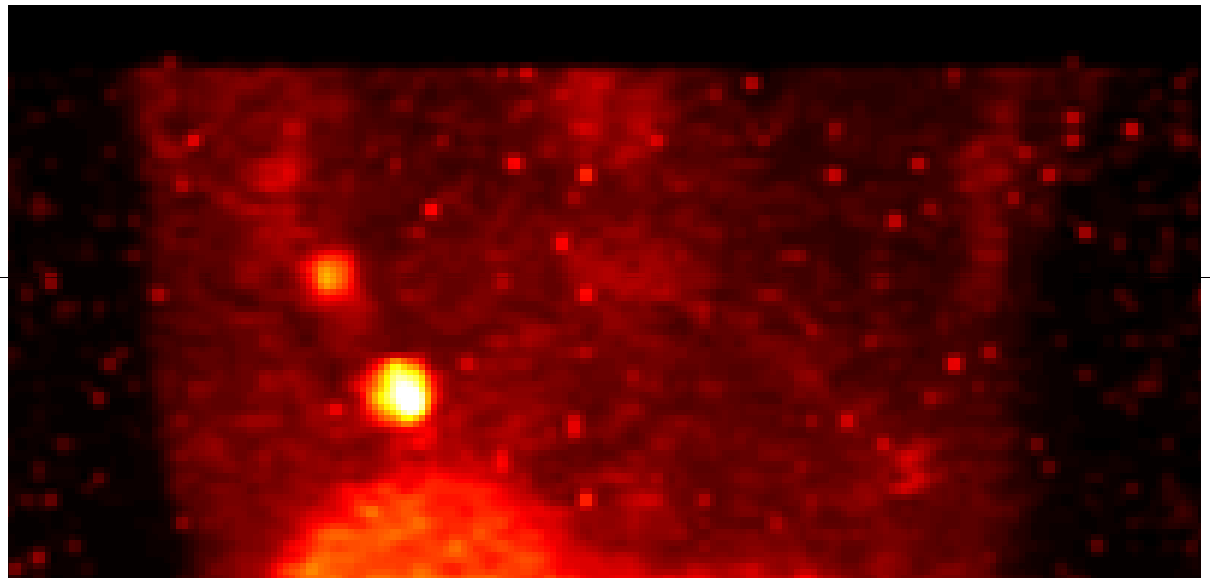

SPECT imaging after injection of 99mTc-RGD peptide

Potential for earlier assessment of response to chemotherapy

- Avoid unnecessary cost and toxicity
- Switch to alternative treatment sooner

THE UNIVERSITY OF TEXAS
MD ANDERSON
CANCER CENTER
Making Cancer History™

Approaches to Optical Imaging of Integrins in Neo-Angiogenesis

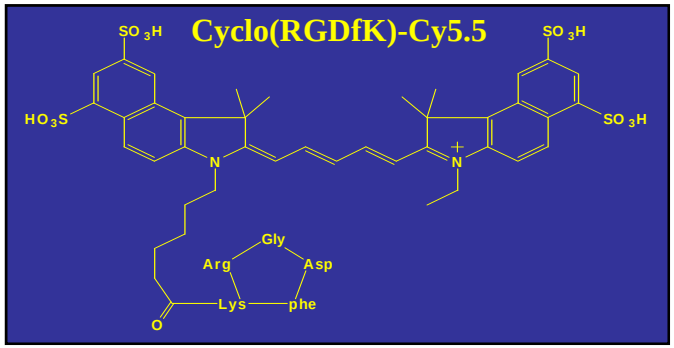

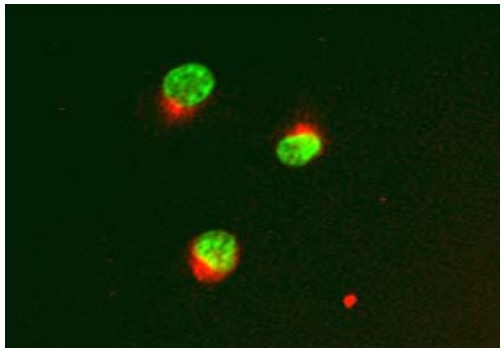

Our pipeline:

- MMP9
- EGFR
- PDGFR
- IL11Rα

RGD-Cy5.5

RGD + RGD-Cy5.5
1 hr interval

Cy5.5

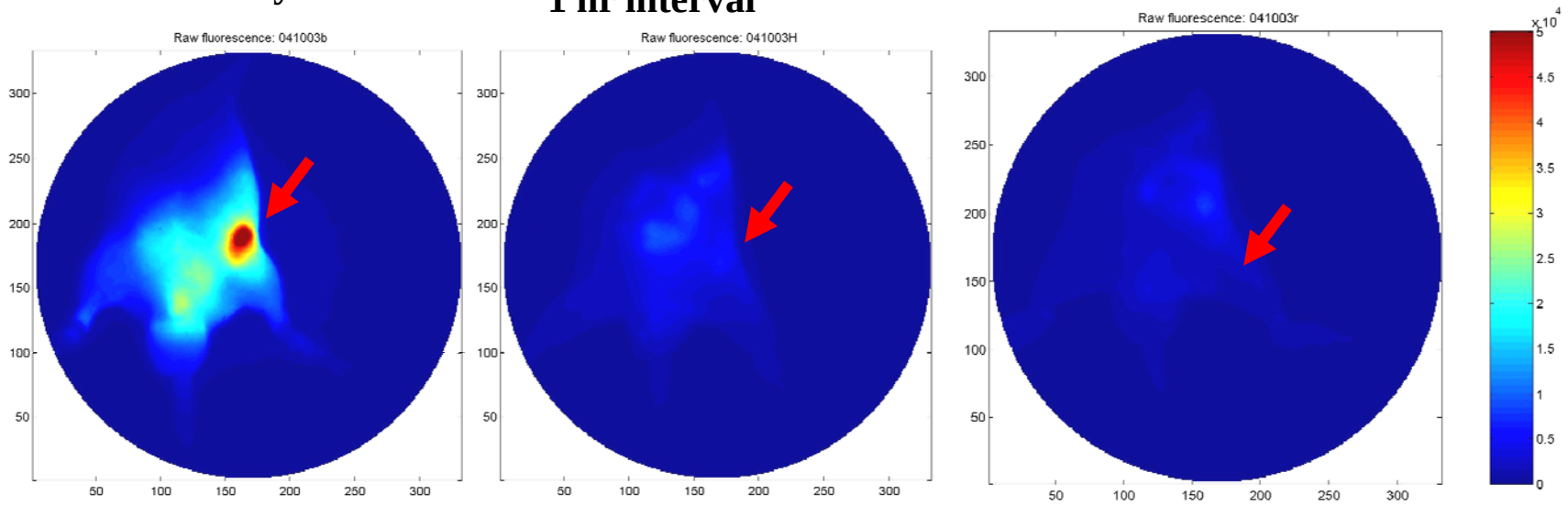

6 nmol/mouse

600 nmol + 6 nmol

30 nmol

THE UNIVERSITY OF TEXAS
MD ANDERSON
CANCER CENTER
Making Cancer History™

Structure of ^{111}In-DTPA-K(IRDye800)-c(KRGDf).

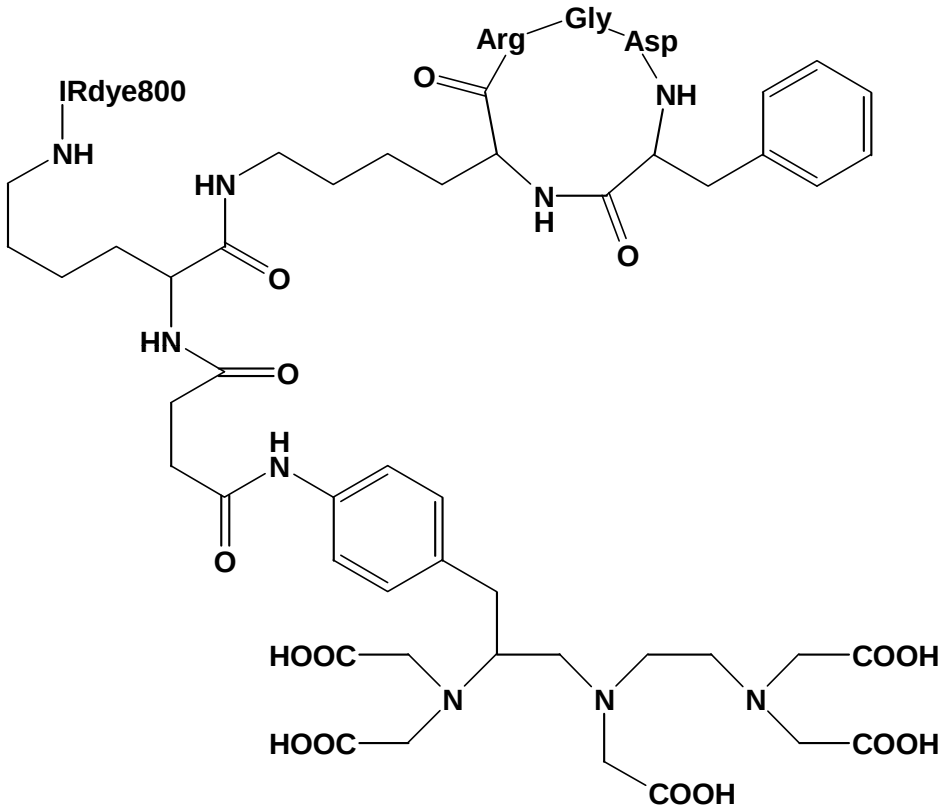

THE UNIVERSITY OF TEXAS
MD ANDERSON
CANCER CENTER
Making Cancer History™

Gamma and near-infrared imaging of 111In-DTPA-K(IRDye800)-c(KRGDf) in nude mice bearing s.c. human melanoma.

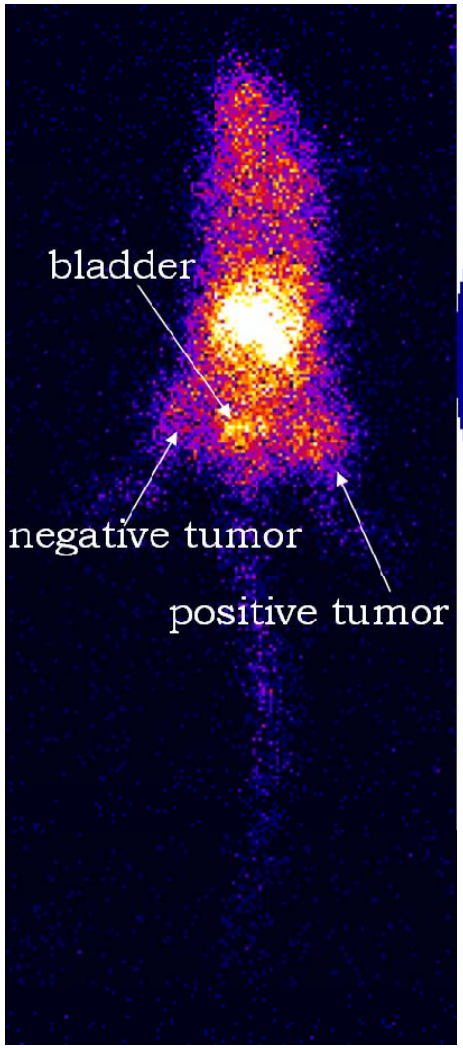

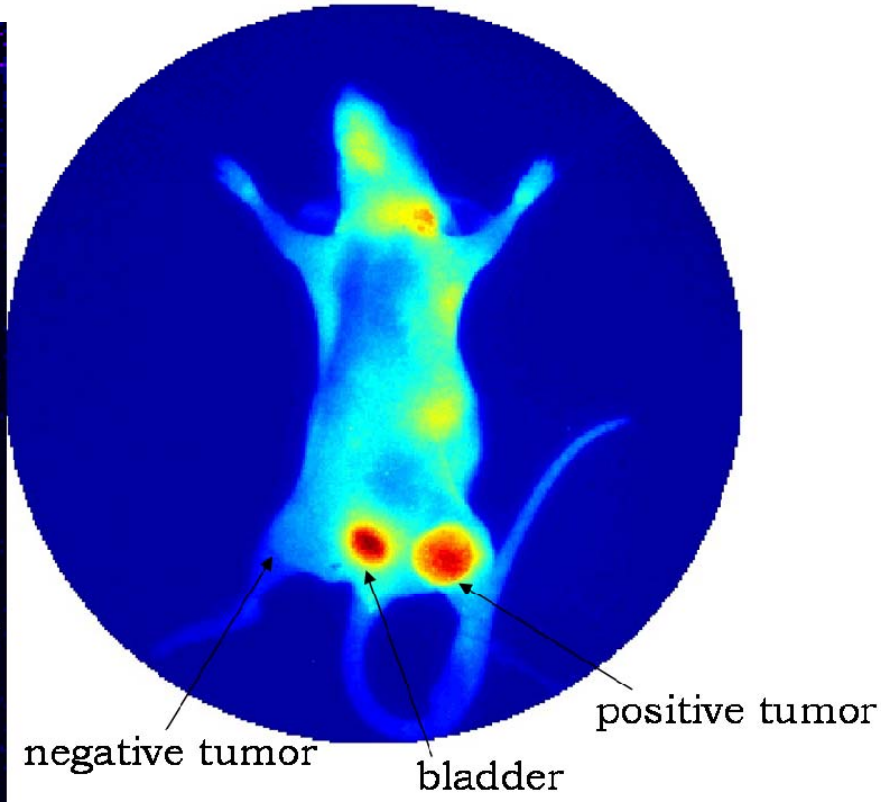

M21 tumor is positive in integrin αVβ3 expression, while M21-L tumor is negative in αVβ3 expression.

THE UNIVERSITY OF TEXAS
MD ANDERSON
CANCER CENTER
Making Cancer History™

Selective accumulation of 111In-DTPA-K(IRDye800)-c(KRGDf) in M21 melanoma tumors that express integrin αVβ3.

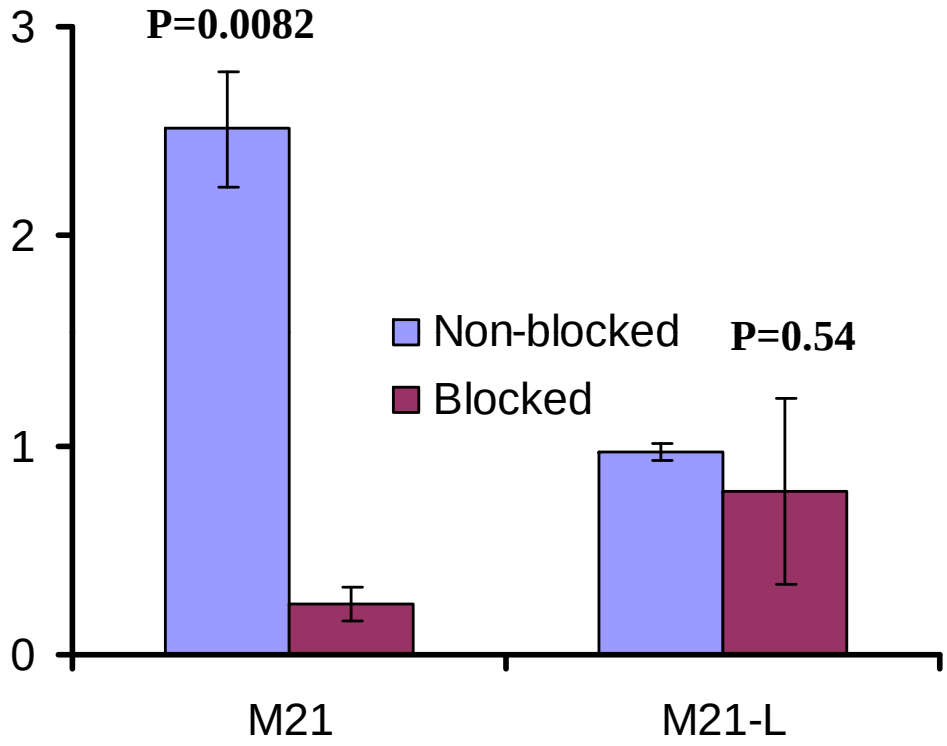

Accumulation of the radiotracer in M21 tumor can be blocked by the parent RGD peptide. On the other hand, preinjection of the parent RGD peptide do not cause significant reduction in the uptake of ^{111}In-DTPA-K(IRDye800)-c(KRGDf) in αvβ3-negative M21-L tumors.

THE UNIVERSITY OF TEXAS
MD ANDERSON
CANCER CENTER
Making Cancer History™

Development of NIR Imaging Probe for Clinical Applications: RGD Conjugates with TS-ICG Dyes

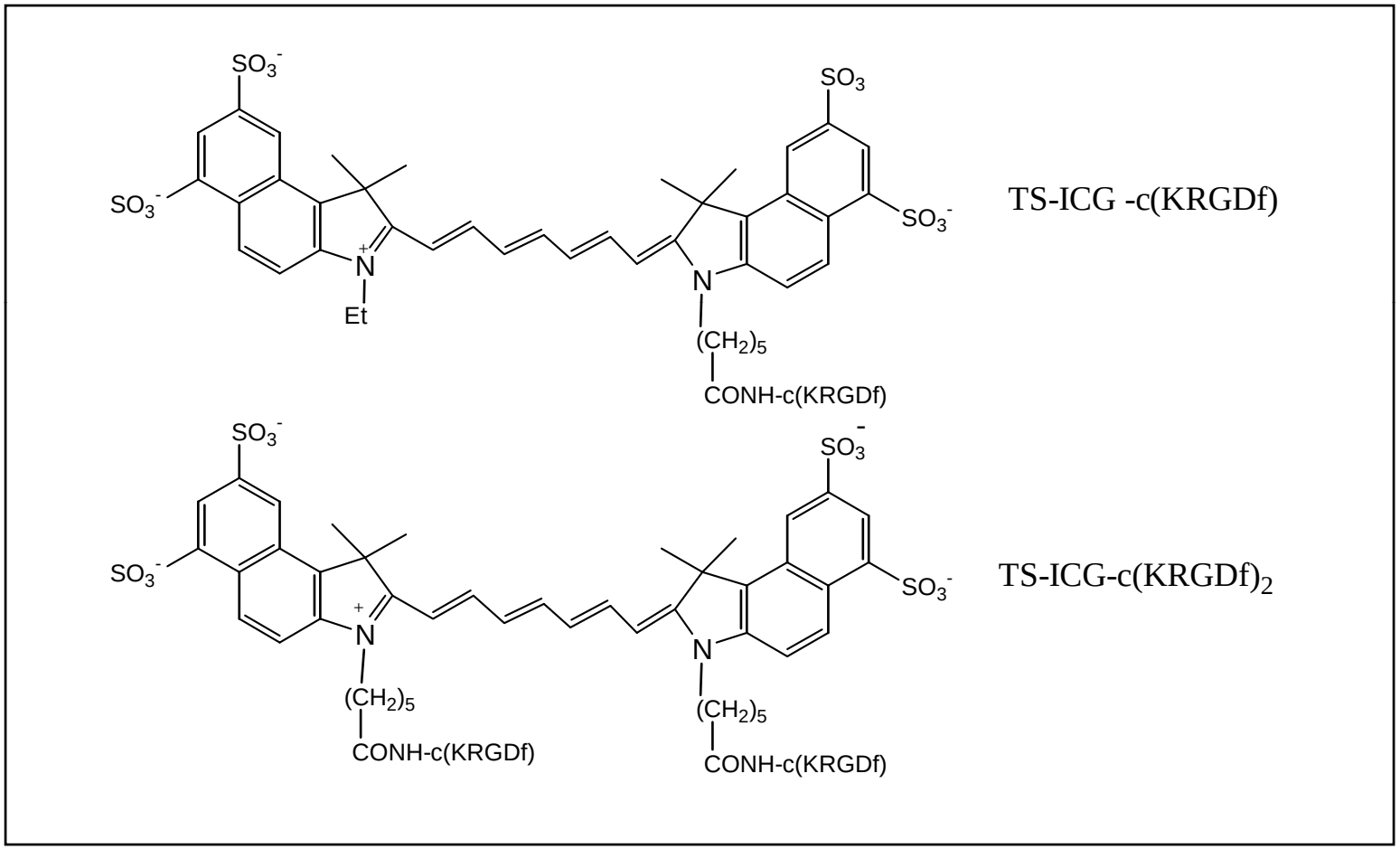

Structures of conjugates of TS-ICG containing one and two molecules of c(KRGDf) peptide. Ex/Em: 765/796 nm

THE UNIVERSITY OF TEXAS
MD ANDERSON
CANCER CENTER
Making Cancer History™

NIR Imaging using Monomeric and Dimeric RGD Conjugates

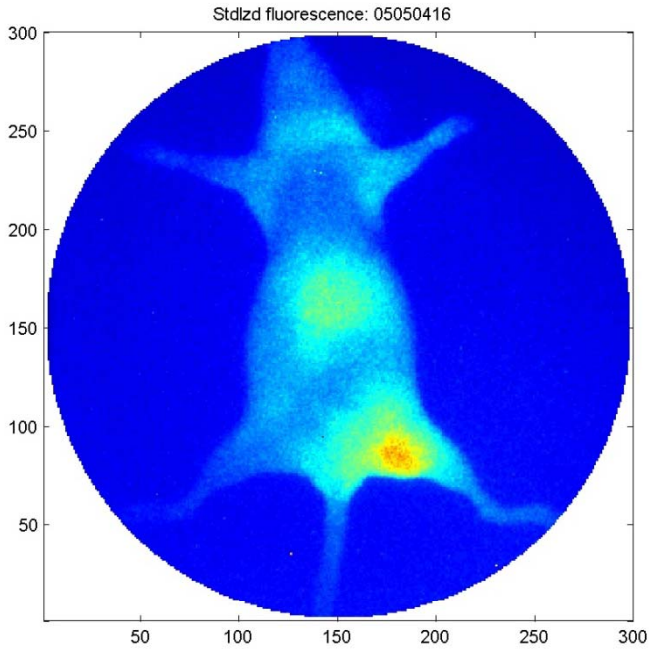

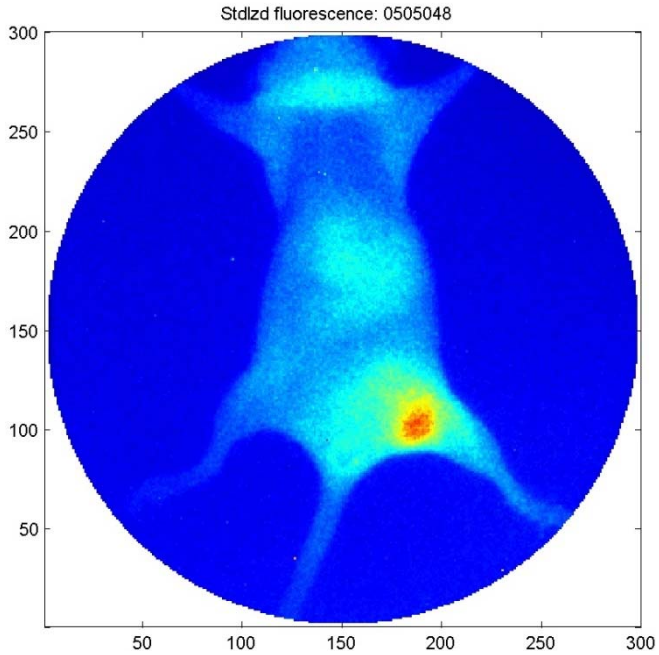

THE UNIVERSITY OF TEXAS
MD ANDERSON
CANCER CENTER
Making Cancer History™

Chemical structure of L-PG-NIR813 or D-PG-NIR813. L- and D-PG-NIR813 differ in their stereoisomeric carbon center (*).

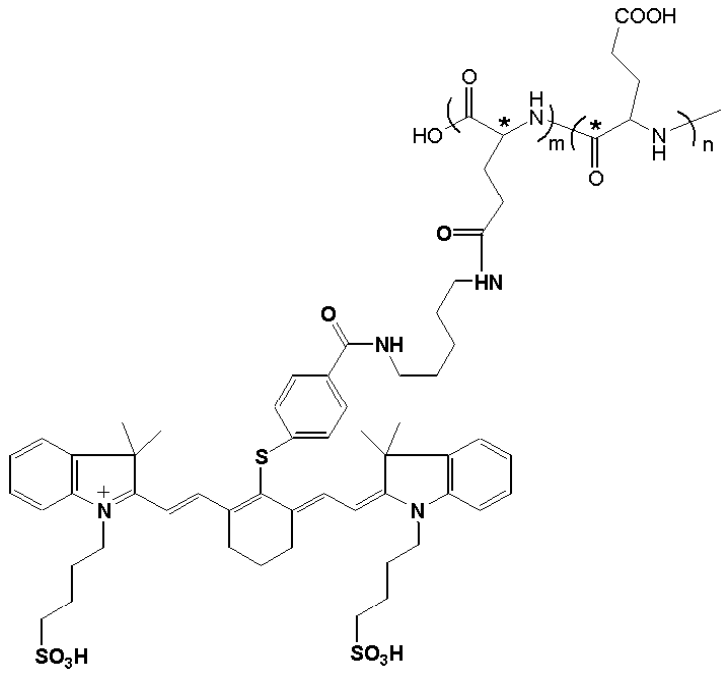

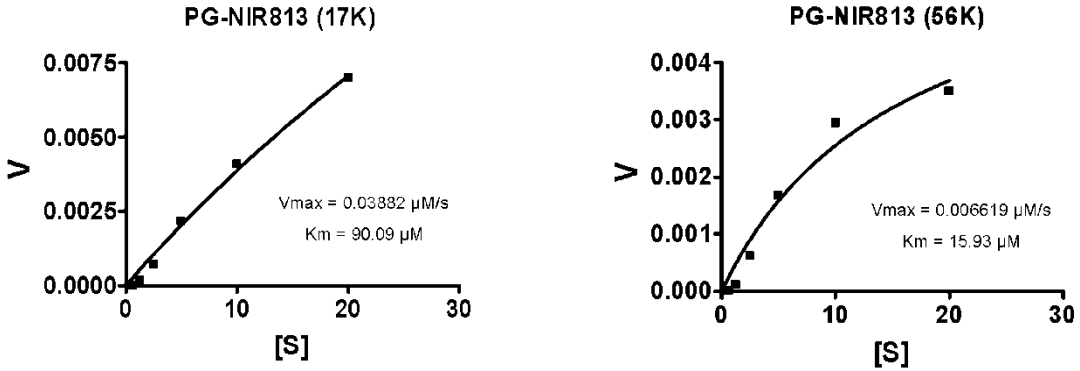

Michaelis-Menten constant s (Km) of the reaction of CB on L-PG-NIR813 with L-PG molecular weight of 17 KD (A) and 56 KD (B).

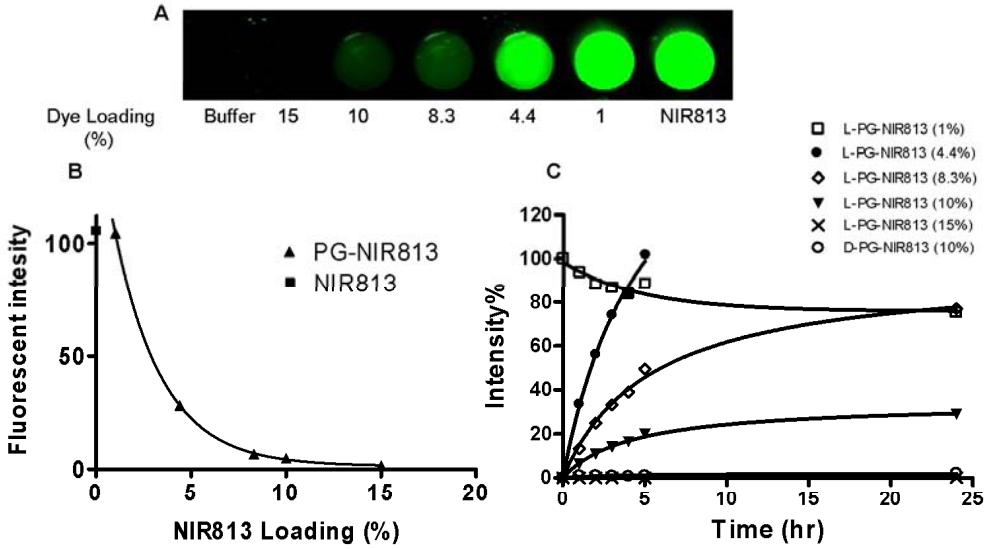

1. ***Quenching efficiency increased with increasing loading of NIR813 (Fig. 2A&B);***
2. ***D-PG-NIR813 and L-PG-NIR813 containing 15% NIR813 could not be activated with CB (Fig. 2C);***
3. ***The optimal loading of NIR813 in L-PG-NIR813 is between 4.4% and 10%.***

THE UNIVERSITY OF TEXAS
MD ANDERSON
CANCER CENTER
Making Cancer History™

Dose-dependent inhibition of CB-mediated degradation of L-PG-NIR813 by specific CB inhibitor (Inhibitor II).

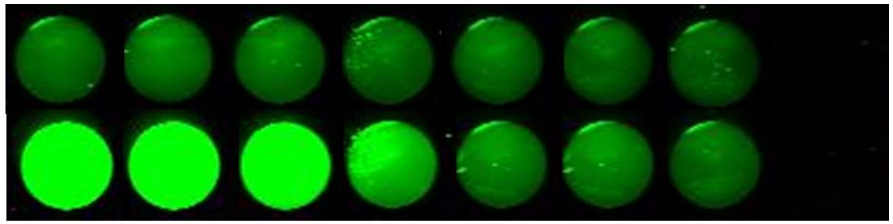

Inhibitor II (μM)	0	0.08	0.38	1.9	9.6	48	240	Ctr

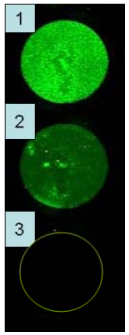

Degradation of PG-NIR813 (8.3% loading) by U87 cells culture for 24 hr (1) and 0 hr (2). Culture medium without cells was used as a control (3).

THE UNIVERSITY OF TEXAS
MD ANDERSON
CANCER CENTER
Making Cancer History™

In vivo imaging after intravenous injection of L-PG-NIR813 into U87(TGL) nude mice.

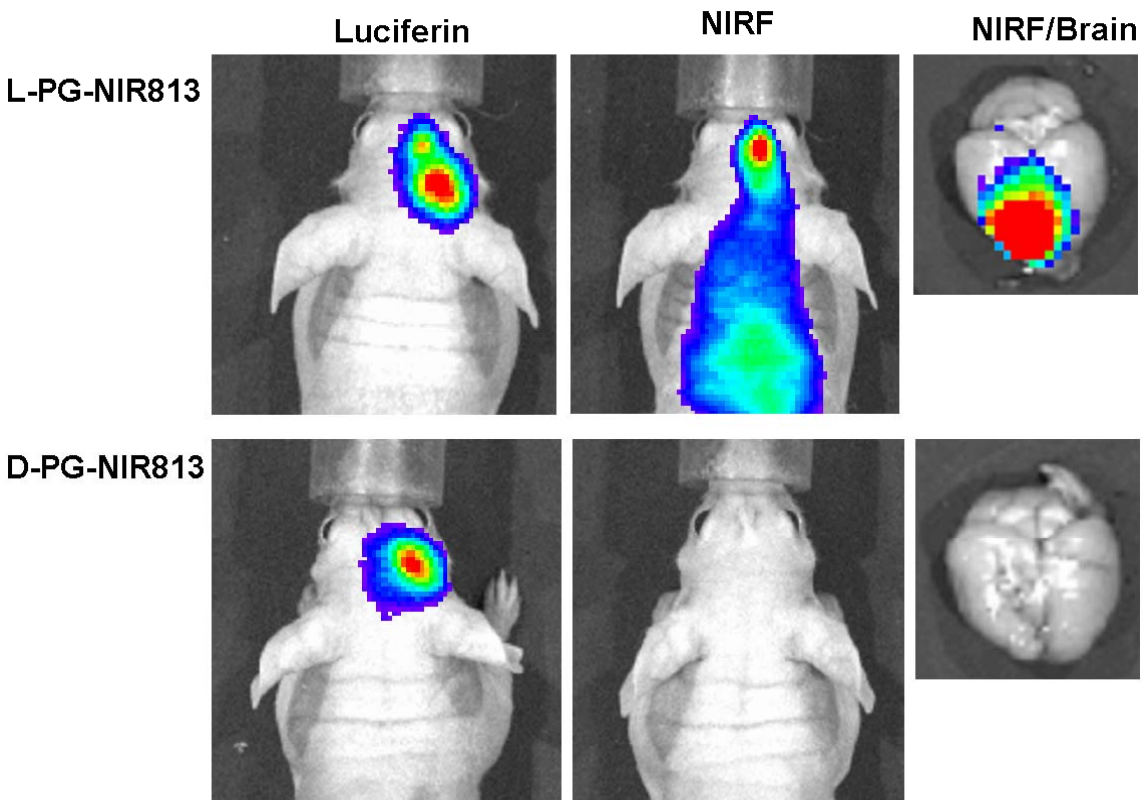

NIRF Images were acquired at 24 hr after i.v. injection of PG-NIR813 (50 nmol/mouse, 17 KD, 8.3 % loading). Note the mouse injection with L-PG-NIR813, but not the mouse injected with D-PG-NIR813, exhibits strong NIRF signal.

THE UNIVERSITY OF TEXAS
MD ANDERSON
CANCER CENTER
Making Cancer History™

Co-localization of PG-GdDTPA-NIR813 with isosulfan blue (A-D).

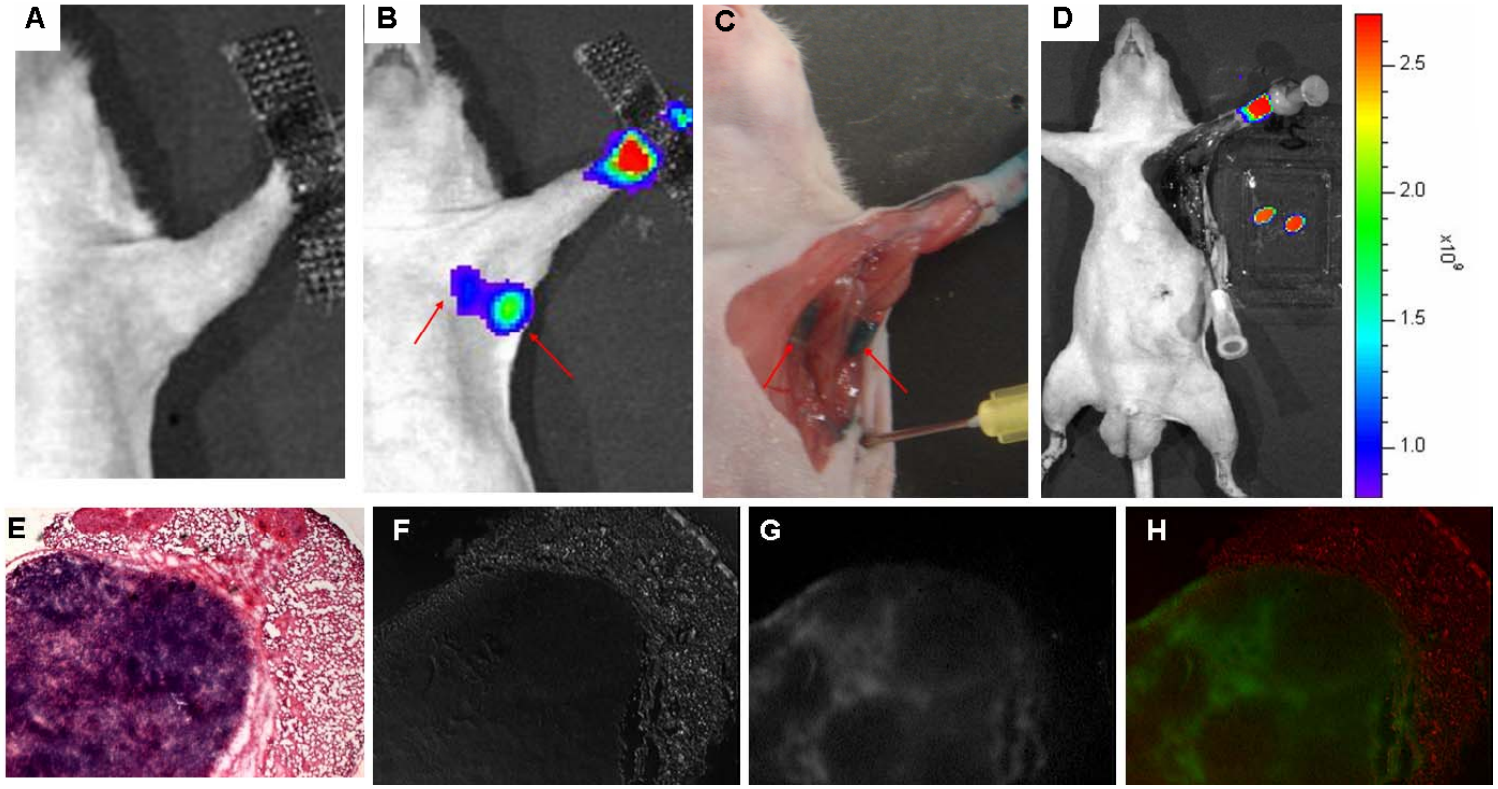

Microphotographs of representative resected lymph node confirming the uptake of PG-GdDTPA-NIR813 in the LN (E-H). E: H&E stained tissue section. F: DIC image. G: NIRF image. H: Overlay of the DIC and NIRF images. NIRF signal is pseudocolored green, and DIC pseudocolored red. Original magnification: 50x.

Dual MR/optical imaging of the axial and branchial lymph nodes in normal athymic nude mice.

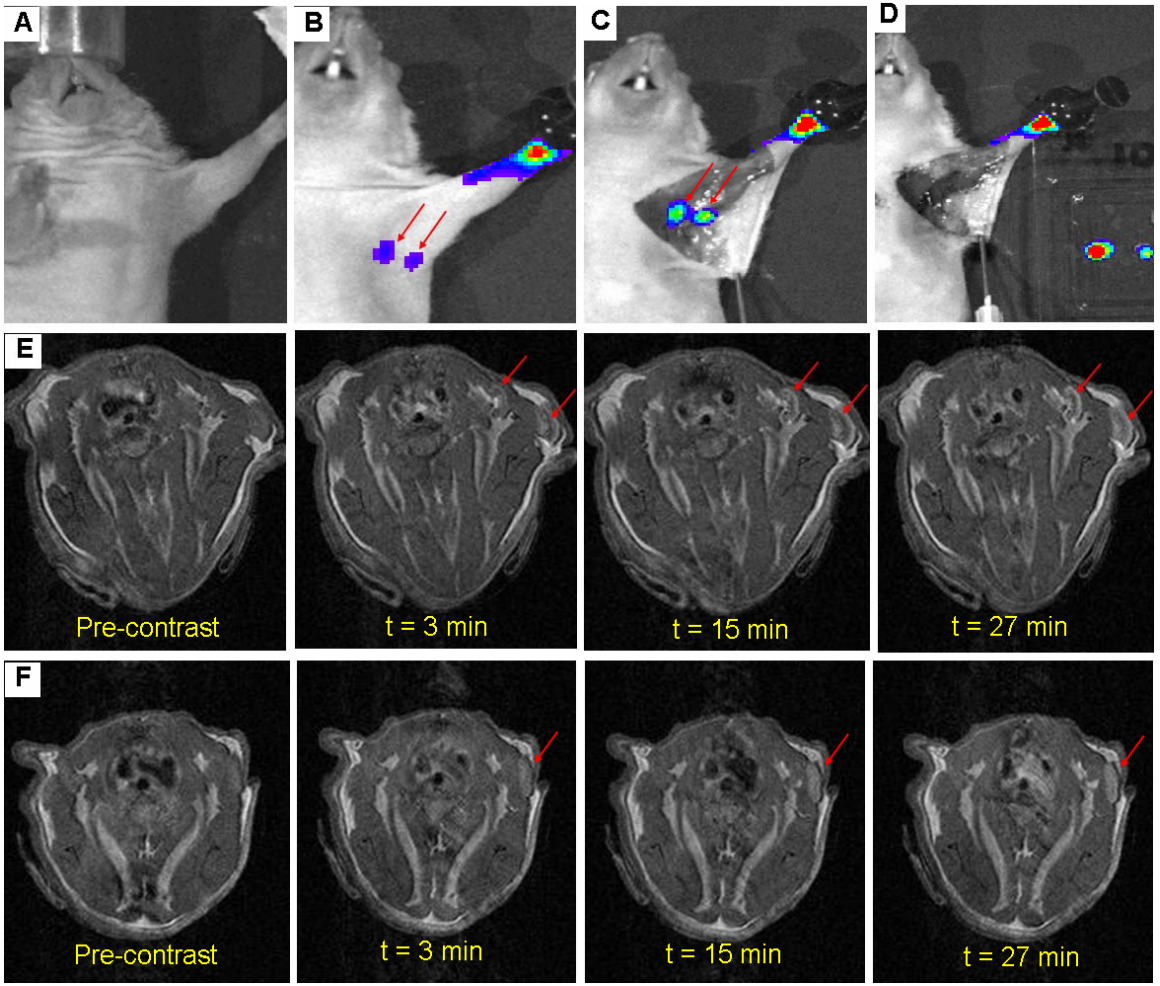

(A) Pre-contrast overlay of white light and NIRF images. (B) Overlay of white light and NIRF images 1 hr after injection of PG-GdDTPA-NIR813 (0.002 mM/L Gd/kg). (C) NIRF image of the same mouse without skin. (D) Resected lymph nodes showed bright fluorescence signal. E-F: Representative T1-weighted axial MR images at different times. PG-GdDTPA-NIR813 was injected at a dose of 0.02 mmol Gd/kg (E) and 0.002 mmol Gd/kg (F). The arrows indicate SLN.

Visualization of cervical lymph nodes after interstitial injection of PG-GdDTPA-NIR813

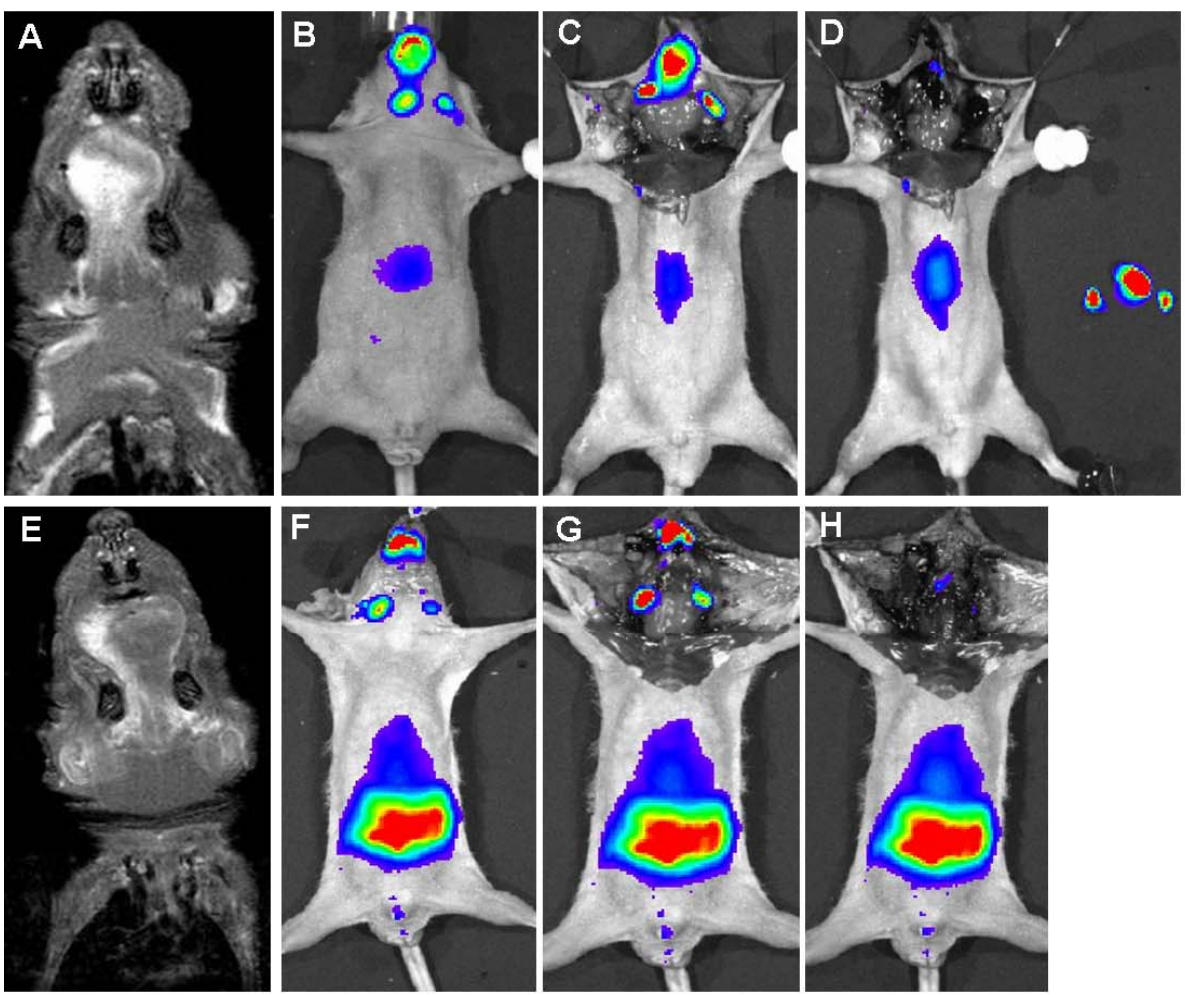

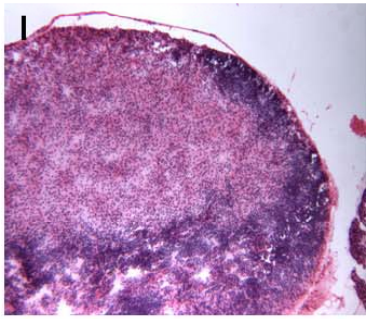

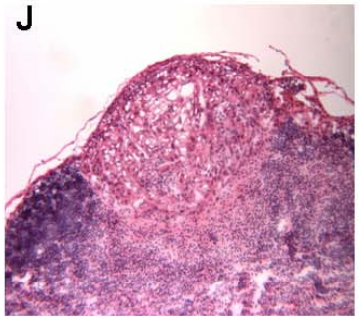

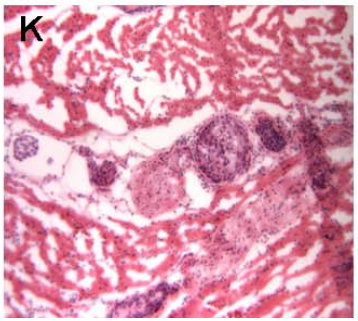

THE UNIVERSITY OF TEXAS MD ANDERSON CANCER CENTER
Making Cancer History™

PG-GdDTPA-NIR813 (0.02 mmol Gd/kg) was injected into the tongue of a normal mouse (A-D) and a mouse with a human DM14 oral squamous carcinoma tumor grown in the tongue (E-H). H&E stained lymph node sections (I-K) indicating the presence of micrometastases (J) and presumably in-transit metastases in lymphatic duct (K). Note the difference in the pattern of lymph node enhancement between normal (A) and metastatic (E) nodes in T1-weighted MRI.

Detection of Tumors by Molecular Imaging of Metabolic Shifts

THE UNIVERSITY OF TEXAS
MD ANDERSON
CANCER CENTER
Making Cancer History™

Comparative PET Imaging of Prostate Carcinomas with ^{18}F-FDG and ^{11}C-Ac

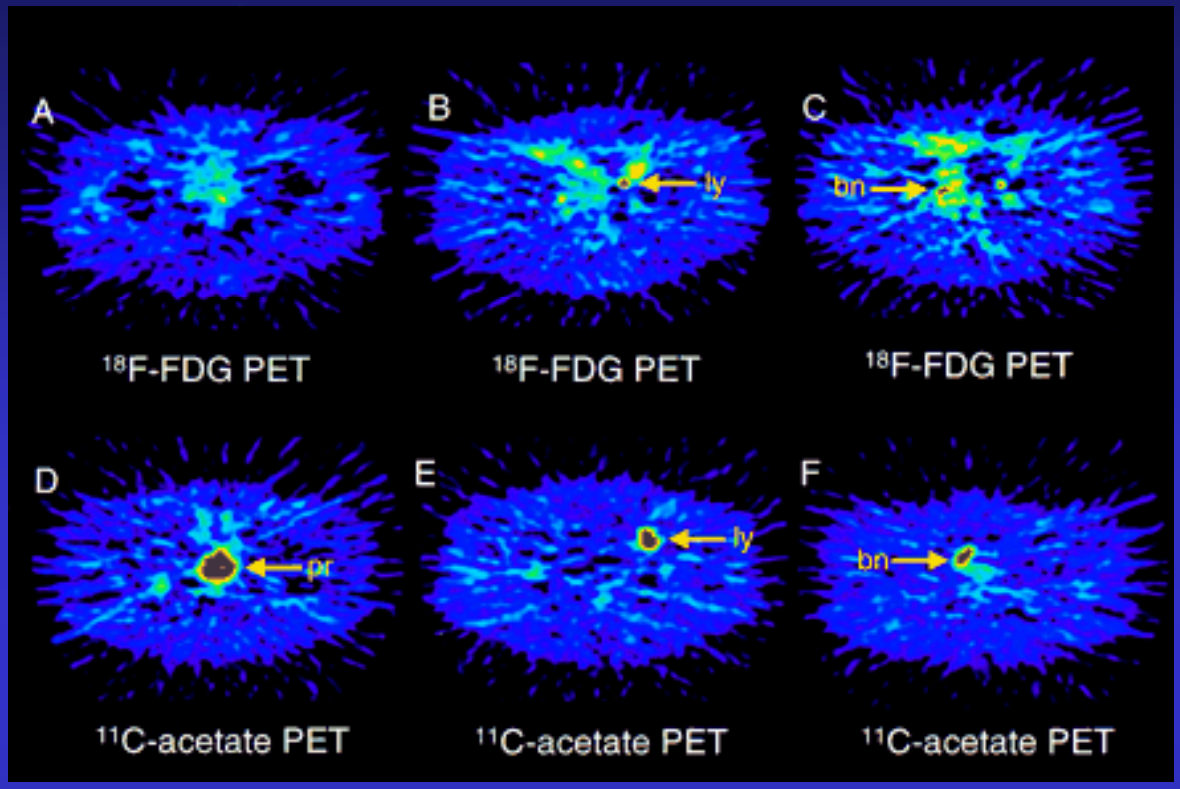

PET images of prostate, lymph node, and bone metastases obtained using ^{18}F-FDG and ^{11}C-Ac from 73-y-old man with poorly differentiated (Gleason sum 7) adenocarcinoma of prostate.

(A) ^{18}F-FDG PET shows low uptake in prostate, with SUV of 2.87.

(B and C) ^{18}F-FDG uptake in left iliac lymph node metastatic lesion (B) and right pubic bone metastatic lesion (C).

(D–F) ^{11}C-Acetate PET shows high uptake in prostate (D), with SUV of 5.45; in left iliac lymph node metastatic lesion (E); and in right pubic bone metastatic lesion (F). bn = bone; ly = lymph node; pr = prostate.

Oyama, et al. J Nucl Med (2002)

THE UNIVERSITY OF TEXAS
MD ANDERSON
CANCER CENTER
Making Cancer History™

Metabolism of Fluoro-Acetate

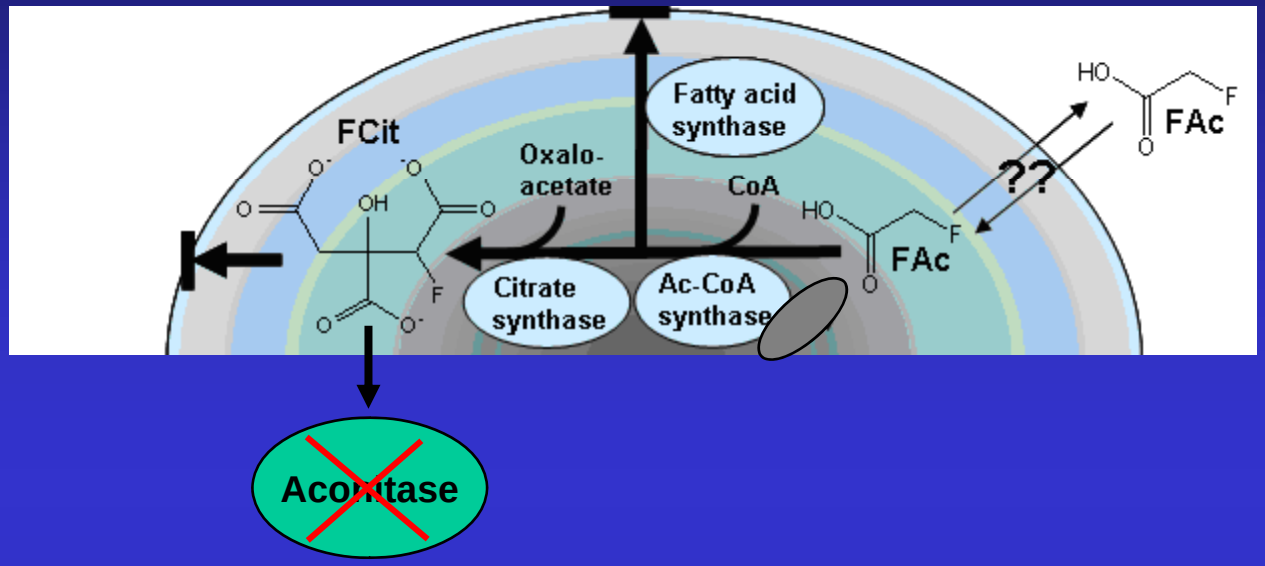

Glycolysis
FDG

Fatty Acid
Synthesis
F-Acetate

THE UNIVERSITY OF TEXAS
MD ANDERSON
CANCER CENTER
Making Cancer History™

In vitro ^{3}H-Acetate and ^{14}C-Fluoroacetate Dual-Label Radiotracer Accumulation Studies in Breast Carcinoma Cell Lines

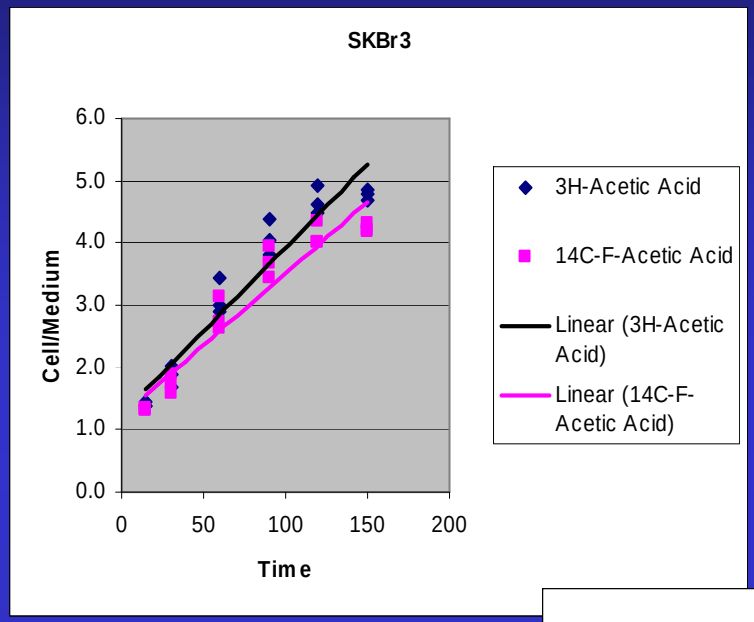

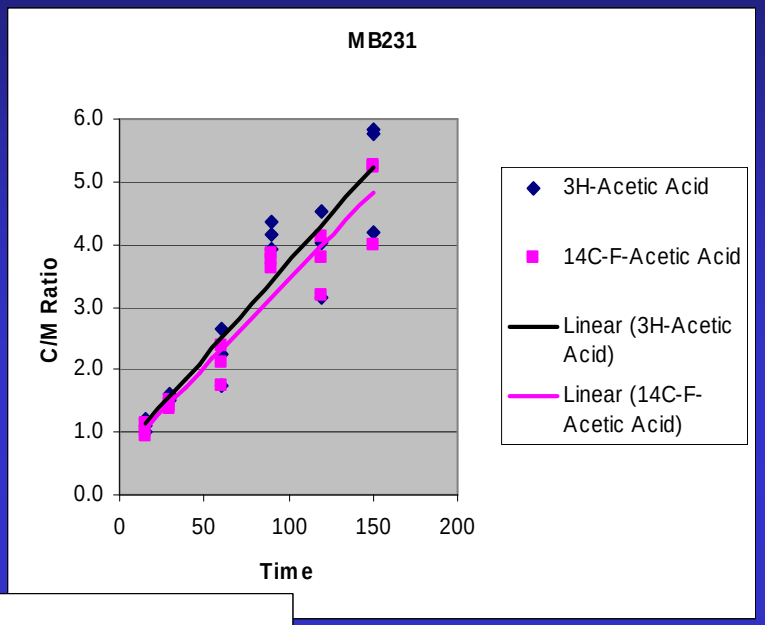

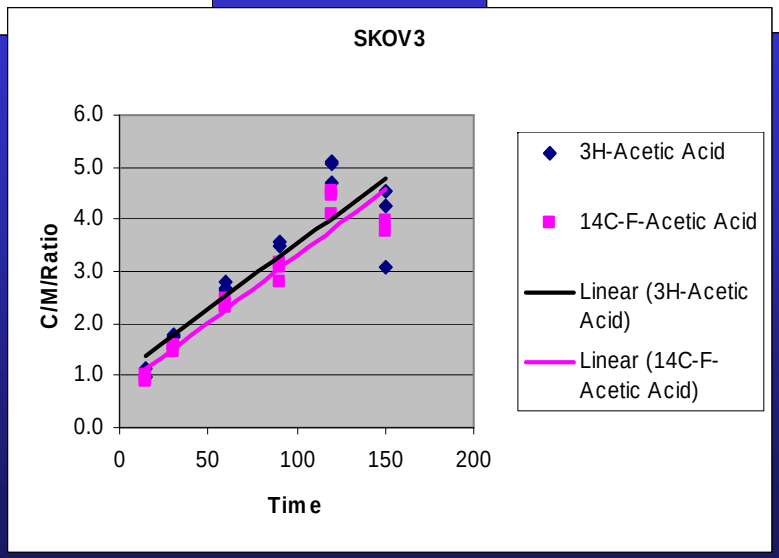

THE UNIVERSITY OF TEXAS
MD ANDERSON
CANCER CENTER
Making Cancer History™

^{18}F-Fluoroacetate in a Multi-Tumor Model

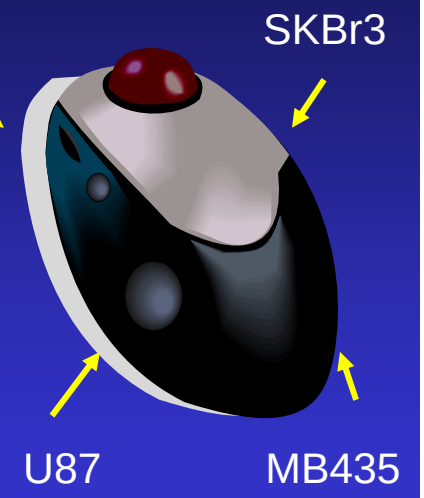

#1

#2

#3

15 min

40 min

60 min

120 min

THE UNIVERSITY OF TEXAS MD ANDERSON CANCER CENTER
Making Cancer History™

Kinetics of [^{18}F]-FAc derived radioactivity accumulation (tumor/muscle ratio) in different tumors

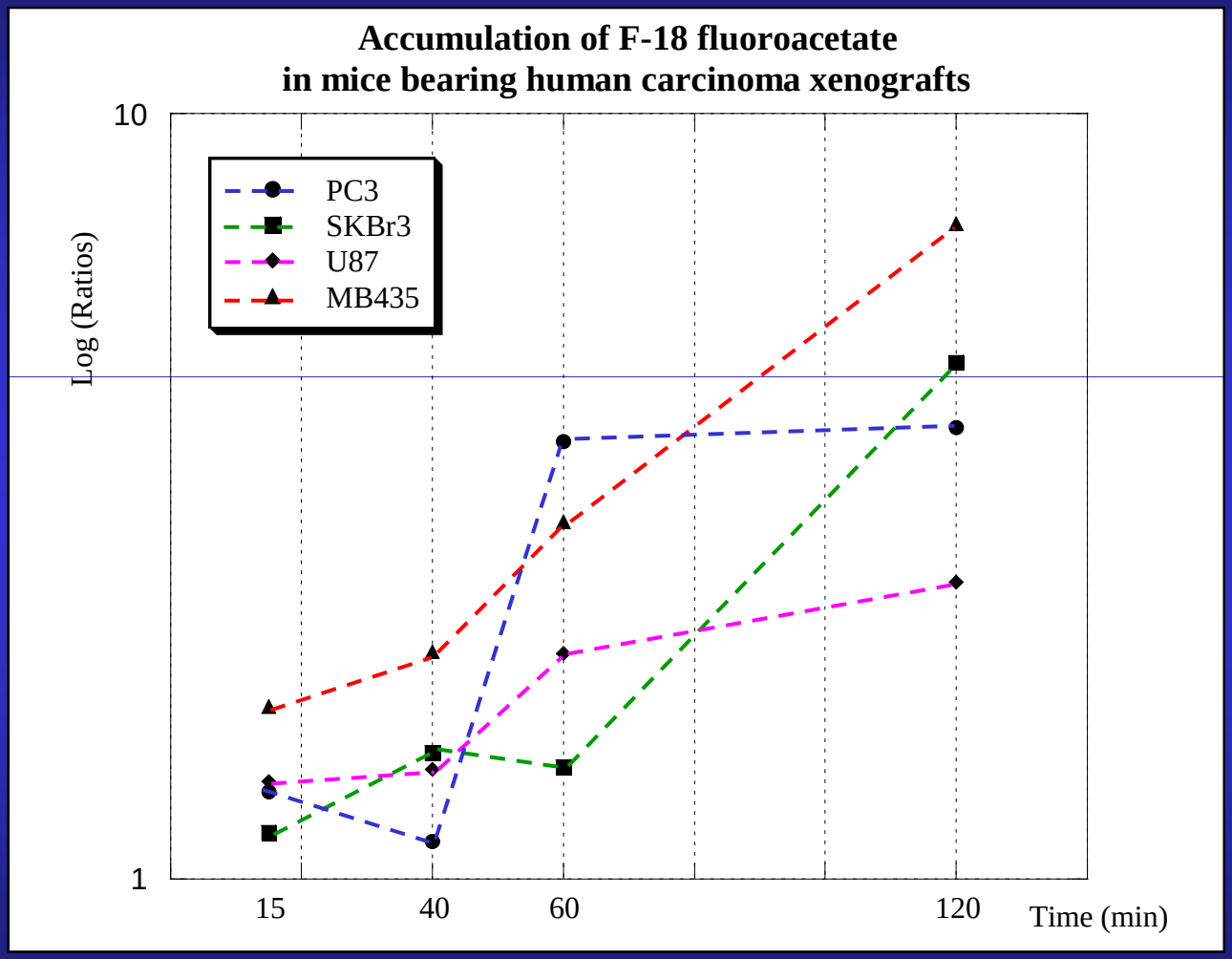

THE UNIVERSITY OF TEXAS
MD ANDERSON
CANCER CENTER
Making Cancer History™

STAGES OF IMAGING AGENT DEVELOPMENT

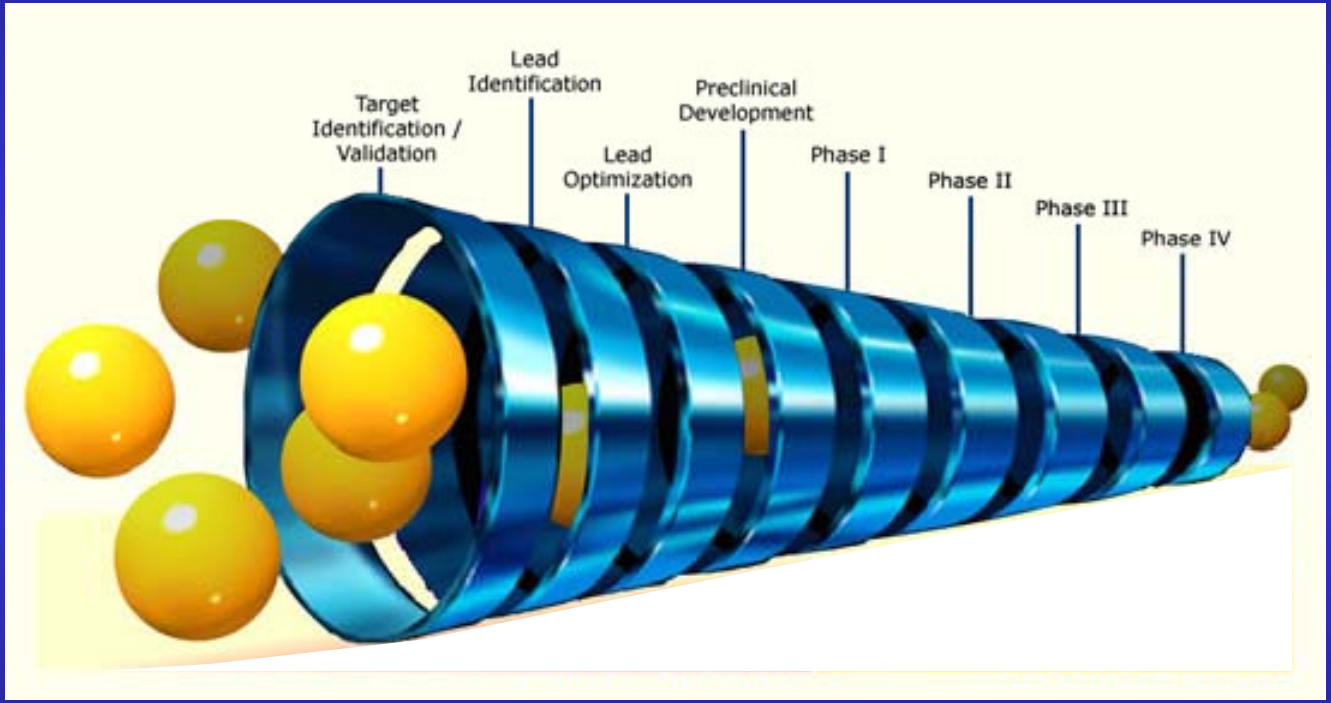

THE UNIVERSITY OF TEXAS MD ANDERSON CANCER CENTER
Making Cancer History™

Dynamic PET/CT Imaging of [^{18}F]-FA

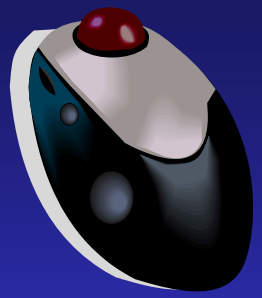

Mouse

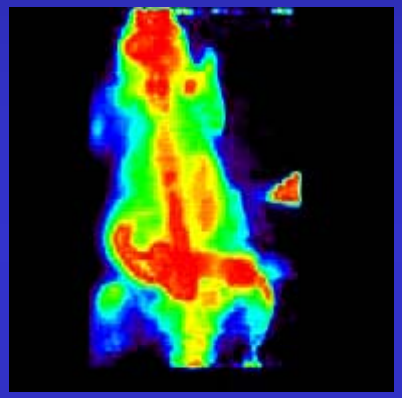

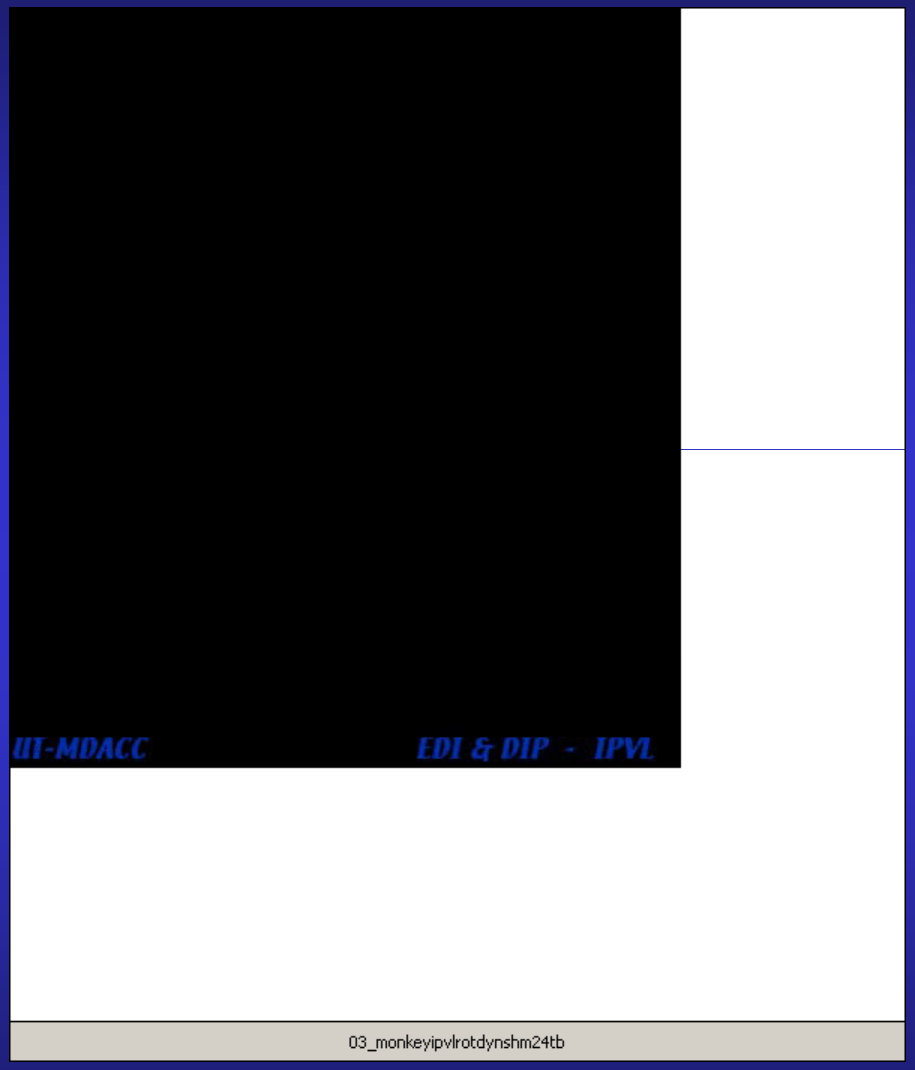

Macaque

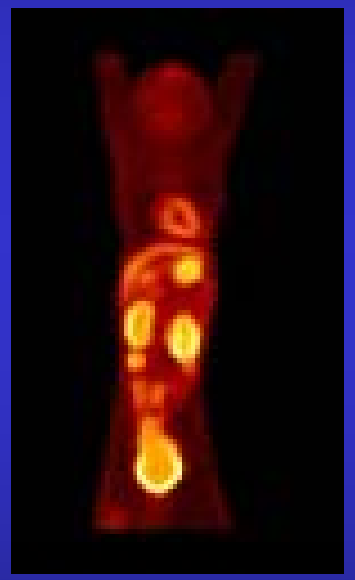

THE UNIVERSITY OF TEXAS
MD ANDERSON
CANCER CENTER
Making Cancer History™

Kinetics of Biodistribution of ^{18}F-FAc in Monkeys

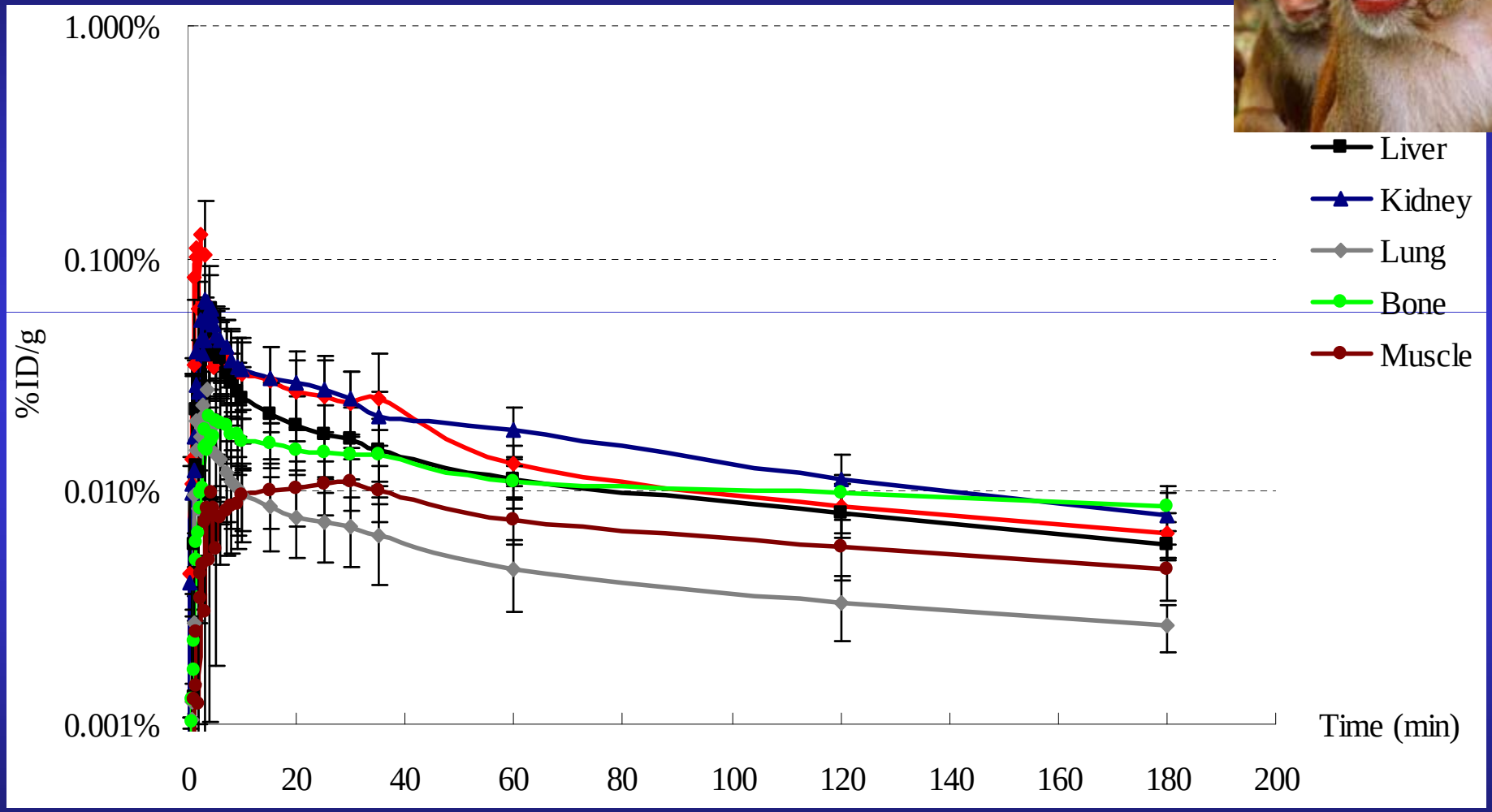

THE UNIVERSITY OF TEXAS
MD ANDERSON
CANCER CENTER
Making Cancer History™

Analysis of Blood Plasma Metabolites

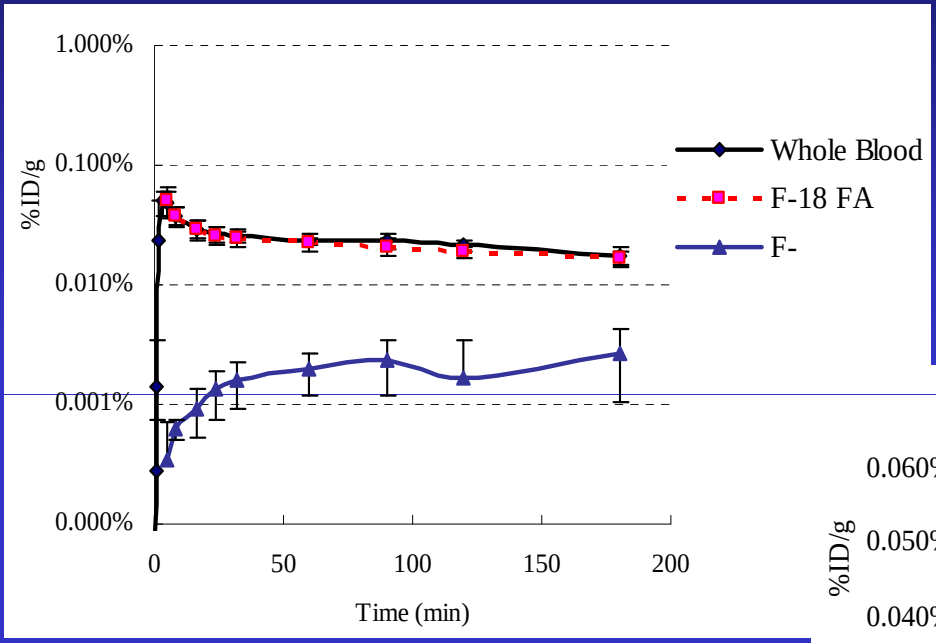

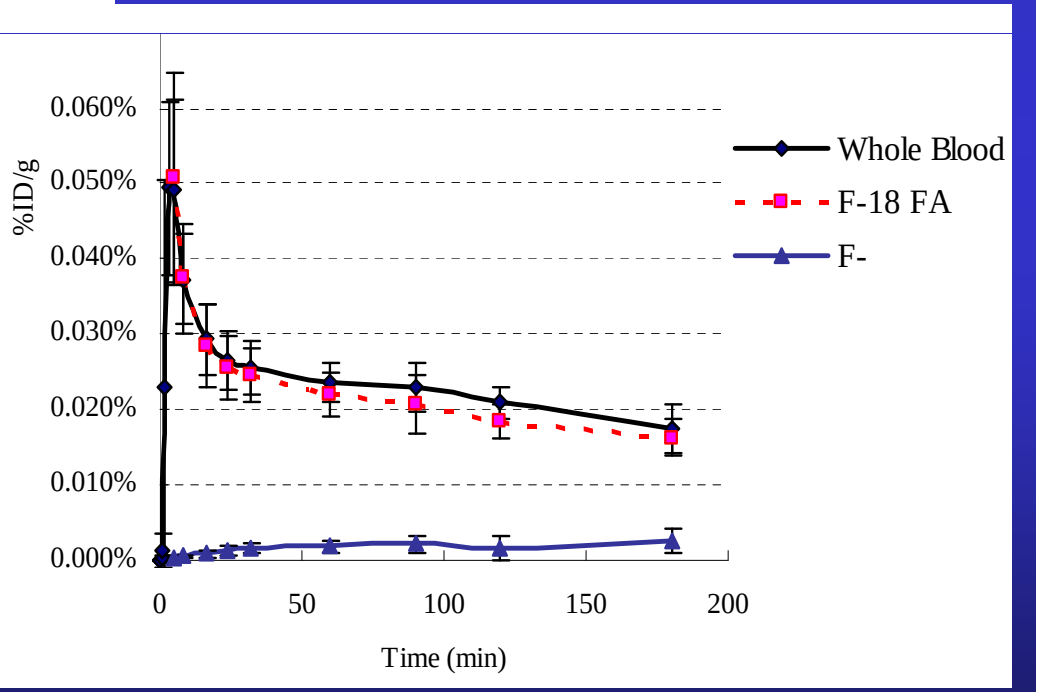

THE UNIVERSITY OF TEXAS
MD ANDERSON
CANCER CENTER
Making Cancer History™

Pharmacological Dose Estimates for [^{18}F]Fluoroacetate

Calculated Specific Activity and Mass.

The total mass per dose and specific activity of ^{18}F-fluoroacetate prepared via no-carrier added synthesis were calculated as follows:

Avogadro's Number	6.02E+23
1Ci in Bq	3.70E+10
Lambda (decay constant)	0.000105022
Molecular weight of the compound	78
Isotope T1/2 (sec)	6600
Dose in mCi	10
N of atoms per dose	3.52306E+12
Moles per dose	5.85E-12
Total weight per dose (g)	4.56E-10
Calculated Sp.Act. (Ci/mol)	1.71E+09

The fluoroacetate used for imaging may have a mass of **0.456 ng** which is about 1/1000 of fluoroacetate that may be present in a cup of tea.

THE UNIVERSITY OF TEXAS MD ANDERSON CANCER CENTER
Making Cancer History™

Phase I study using PET/CT with 18F-FAcetate in Tumors that don't avidly accumulate FDG

- **Prostate carconoma, lymph node mets**
- **Breast carcinoma, lobular, lymph node mets**
- **Brain tumors, GBM**

30 patients (10 patients per tumor type)

Primary objectives:

Pharmacokinetics
Radiolabeled metabolites
Biodistribution
Radiation dosimetry
Dose optimization

Secondary objectives:

Feasibility of tumor detection
as compared to CT and MRI or biopsy

THE UNIVERSITY OF TEXAS MD ANDERSON CANCER CENTER
Making Cancer History™

TUMOR DETECTION:

NEW IMAGING AGENTS

FOR

STROMAL BIOMARKERS

THE UNIVERSITY OF TEXAS
MD ANDERSON
CANCER CENTER
Making Cancer History™

Pancreatic Carcinoma: Problems in Diagnosis & Therapy

- **Pancreatic cancer patients seldom exhibit disease-specific symptoms until late in the course of the disease process**

- **Despite significant advances in the treatment of many other human tumors, the 5-year survival rate in pancreatic cancer remains <5%.**

- **At present, no imaging modality is sensitive for visualization of early stage pancreatic carcinomas or small metastases in the lymph nodes, peritoneum, and on the surface or within the liver.**

- **Novel biomarker screening and diagnostic imaging methods for potential earlier detection and localization of pancreatic carcinomas must be developed in conjunction with new image-guided therapies that would eradicate early neoplastic lesions if survival from this disease is to be improved.**

Current understanding of the molecular changes in the multi-step progression model of pancreatic adenocarcinoma

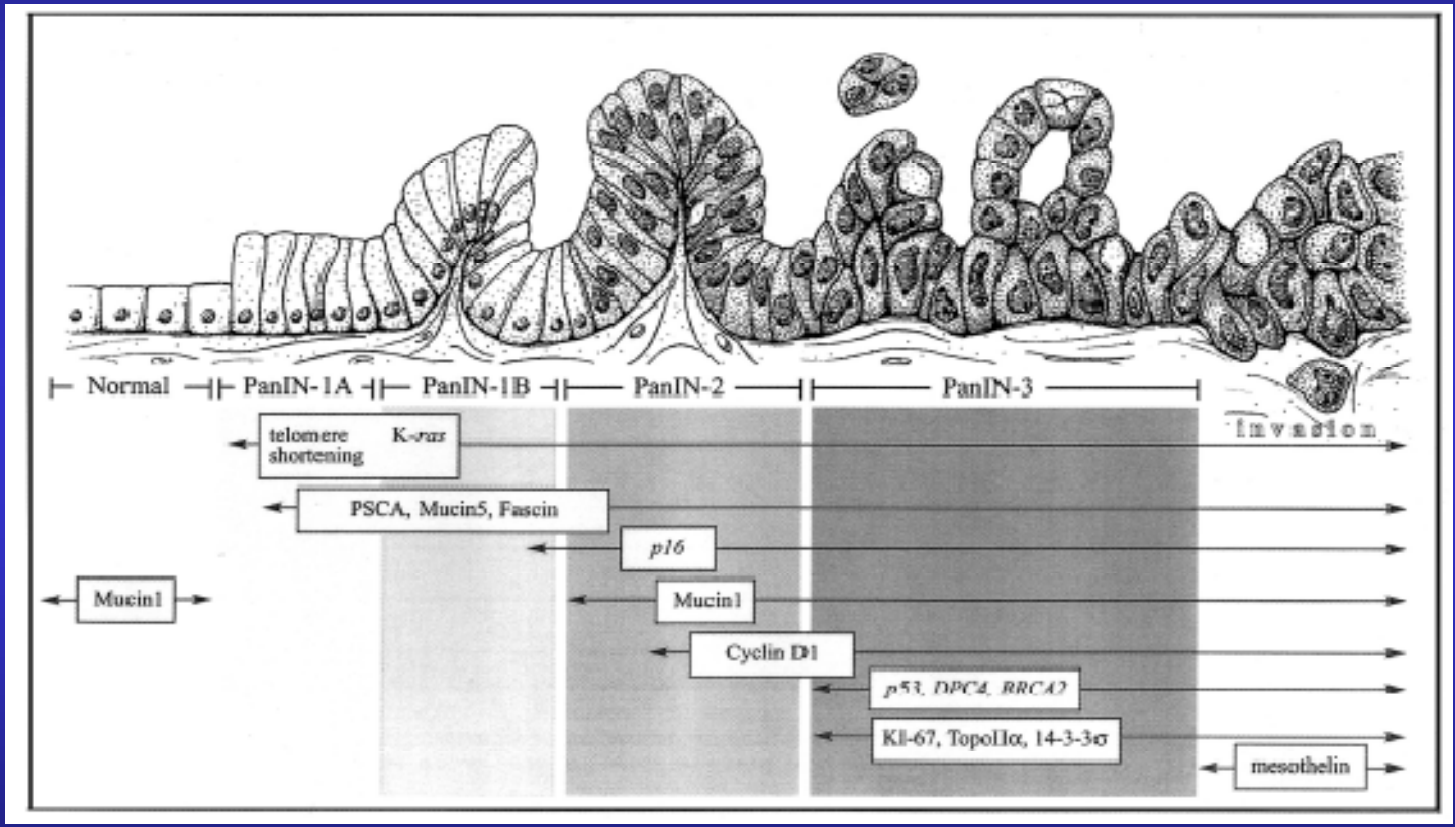

THE UNIVERSITY OF TEXAS MD ANDERSON CANCER CENTER
Making Cancer History™

Molecular Imaging of Stromal Biomarkers: Volume Amplification Approach

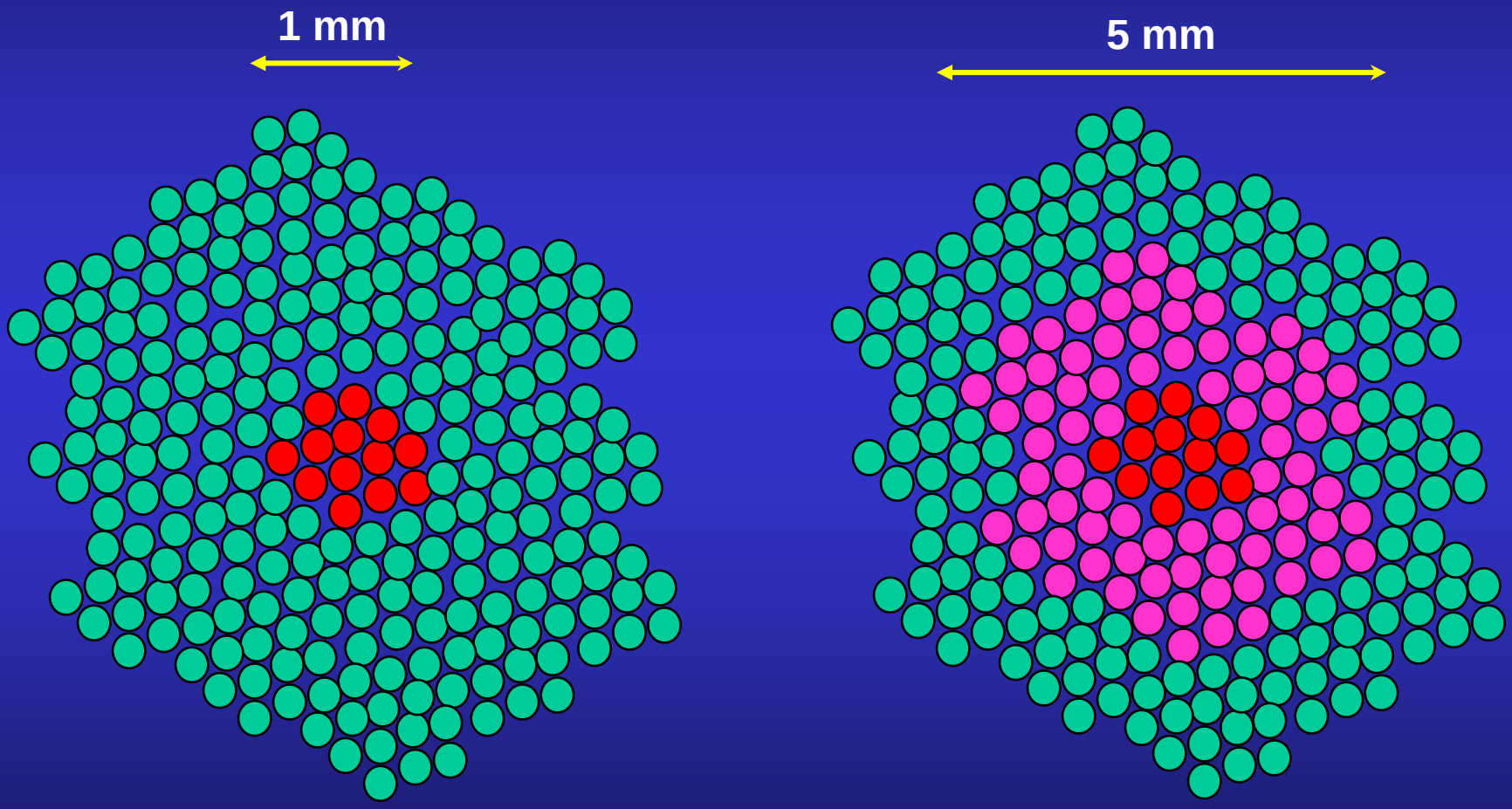

THE UNIVERSITY OF TEXAS
MD ANDERSON
CANCER CENTER
Making Cancer History™

Gene Expression in parenchyma adjacent to infiltrating pancreatic ductal adenocarcinoma and chronic pancreatitis

(Fukushima, et al. Mod Pathol 18, 779-787, 2005)

Gene bank	*Gene name*	*PC (fold change) compared to*	
		NP-P	*CP-P*
(1) NM_002580.1	Pancreatitis-associated protein (HIP/PAP)[a]	130.6	9.9
(2) NM_002343.1	Lactotransferrin (LTF)[a]	40.6	3.1
(3) M80927.1	Human Cartilage glycoprotein-39 (HC-gp39)[a]	18.2	6.8
(4) NM_006507.1	Regenerating islet-derived 1 beta (pancreatic stone protein, pancreatic thread protein) (REG1B)	17.3	7.1
(5) NM_006508.1	Rat regenerating islet-derived-like, human homolog (REGL)	14.8	15.2
(6) NM_018295.1	*Homo sapiens* hypothetical protein FLJ11000 (FLJ11000)	10.7	8.5
(7) NM_018234.1	*Homo sapiens* hypothetical protein FLJ10829 (FLJ10829)	7.7	3.6
(8) NM_021871.1	Fibrinogen, A alpha polypeptide (FGA), transcript variant alpha	7.3	8.5
(9) NM_020997.1	Left–right determination, factor B (LEFTB)	6.7	4.2
(10) NM_001085.2	Serine (or cysteine) proteinase inhibitor, clade A (alpha-1antiproteinase, antitrypsin), member 3 (SERPINA3)	6.2	3.6
(11) NM_000715.1	Complement component 4-binding protein, alpha (C4BPA)[a]	5.6	4.1
(12) NM_001022.1	Ribosomal protein S19 (RPS19)	5	4.4
(13) NM_001871.1	Carboxypeptidase B1 (tissue) (CPB1)	5	3.3
(14) NM_003761.1	Vesicle-associated membrane protein 8 (endobrevin) (VAMP8)	4.6	6.6
(15) BC006134.1	*Homo sapiens*, clone MGC:13053	4.3	11.3
(16) NM_015849.1	Pancreatic elastase IIB (LOC51032)	3.8	6.7
(17) NM_006994.2	Butyrophilin, subfamily 3, member A3 (BTN3A3)	3.6	4.3
(18) NM_000096.1	Ceruloplasmin (ferroxidase) (CP)	3.5	3.3
(19) NM_017422.2	Calmodulin-like skin protein (CLSP)	3.3	4.3
(20) AB018580.1	hluPGFS (3-alpha hydroxysteroid dehydrogenase, type II)	3.3	3.6

[a]The results were confirmed by quantitative RT-PCR.
CP-P: parenchyma adjacent to chronic pancreatitis; NP-P: parenchyma from normal pancreas; PC: pancreatic cancer.

THE UNIVERSITY OF TEXAS MD ANDERSON CANCER CENTER
Making Cancer History™

Synthesis of [^{18}F]-Lactose

Synthesis of a precursor

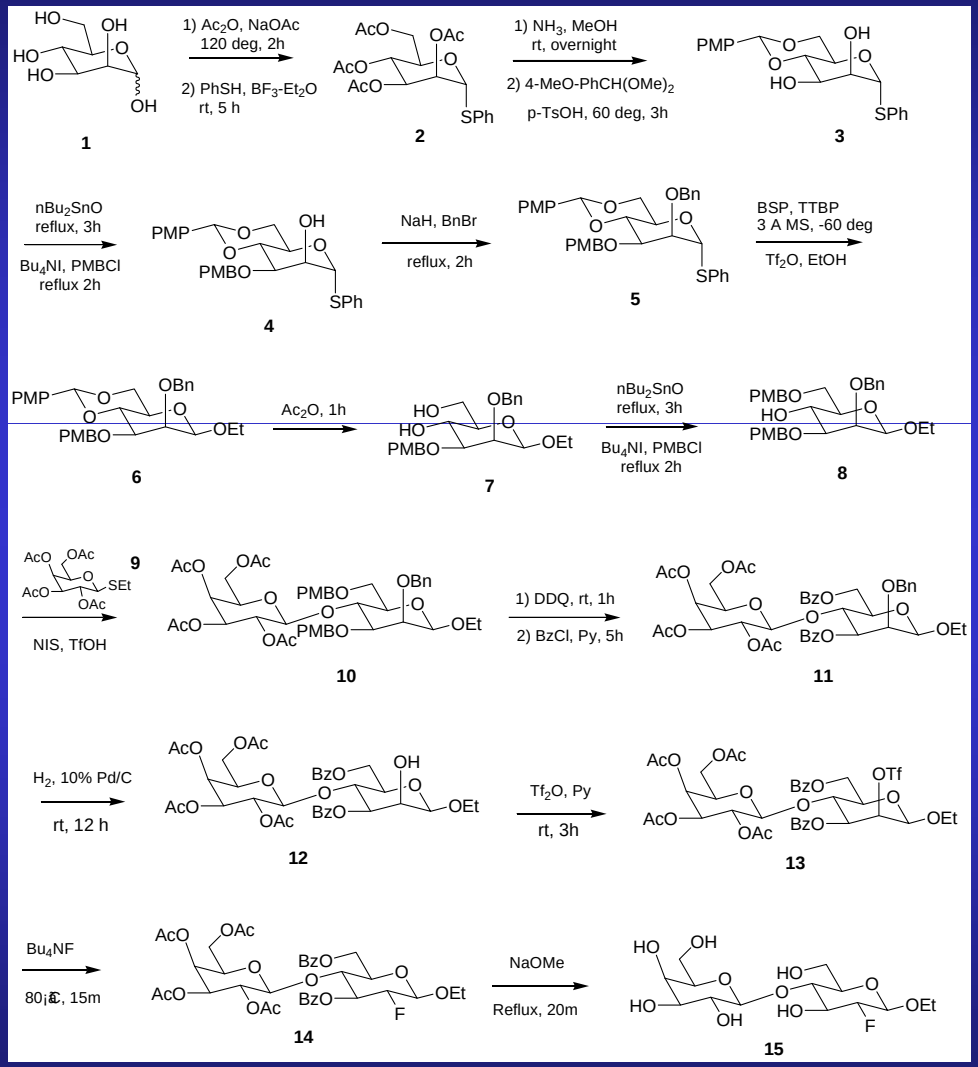

Radiolabeling of [^{18}F]-Lactose

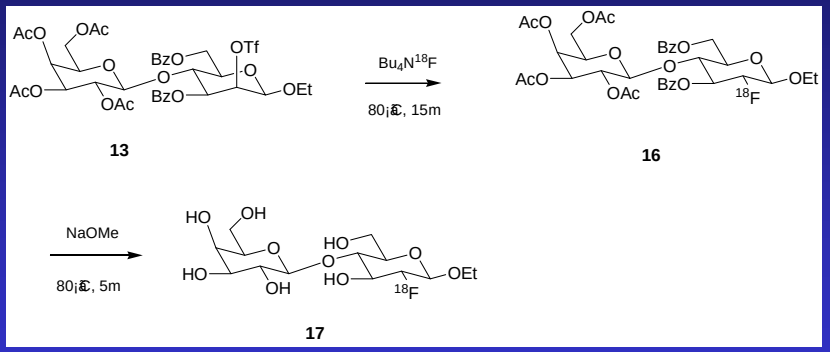

Co-injection of purified 16 with cold version of 14

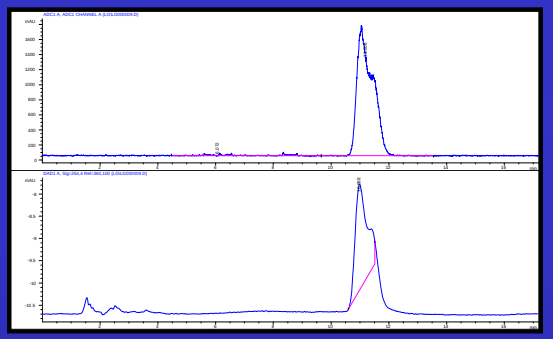

QC Chromatogram of compound 17

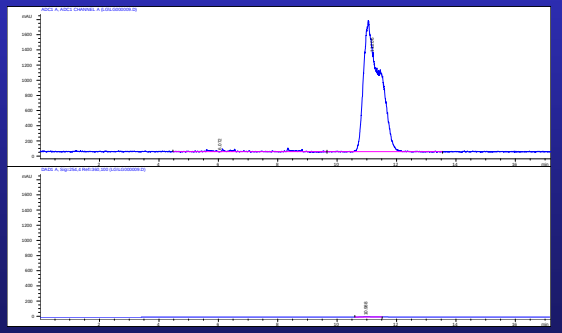

THE UNIVERSITY OF TEXAS MD ANDERSON CANCER CENTER
Making Cancer History™

PET imaging of pancreatic carcinoma

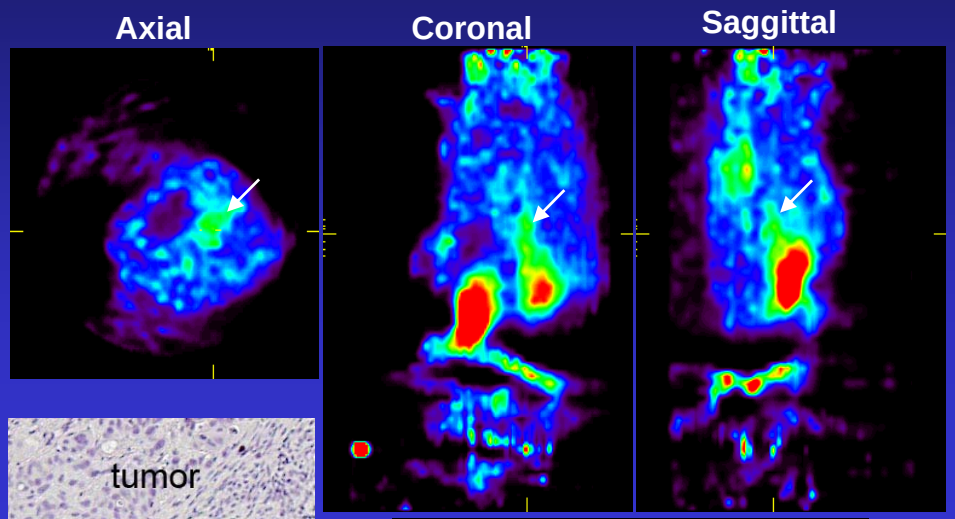

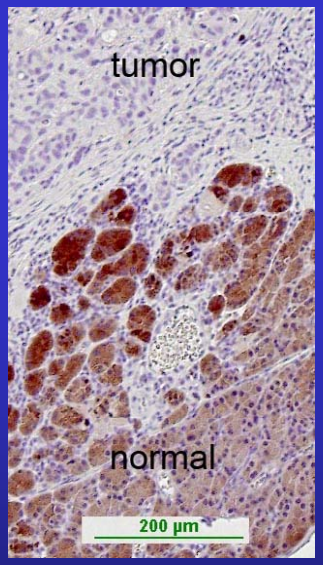

PAP immunostain provided by Dr. Craig Logsdon, MDACC

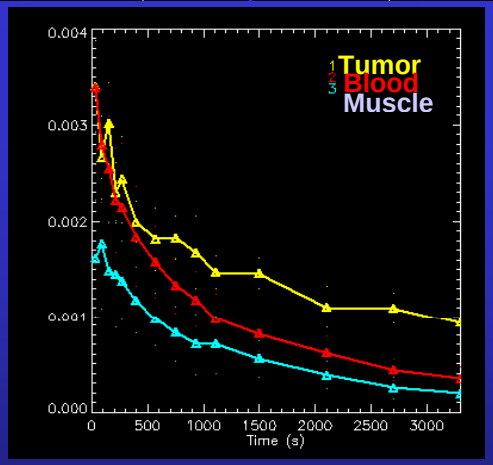

Time-activity curves

PET imaging of mice bearing orthotopic MPanc96 human pancreatic cacinoma xenografts demonstrated higher retention of [^{18}F]FDL (100 uCi i.v.) in the tumor-invaded pancreas, which corresponded with high levels of HIP/PAP protein expression in the peritumoral pancreatic tissue, as evidenced by comparative immunohistochemical analysis in situ. The [^{18}F]FDL was eliminated via the renal clearance.

THE UNIVERSITY OF TEXAS MD ANDERSON CANCER CENTER
Making Cancer History™

Molecular Imaging of Drug Target Expression-Activity: Selection of Therapy

THE UNIVERSITY OF TEXAS
MD ANDERSON
CANCER CENTER
Making Cancer History™

Current Diagnostic – Therapeutic Paradigm

PET/CT

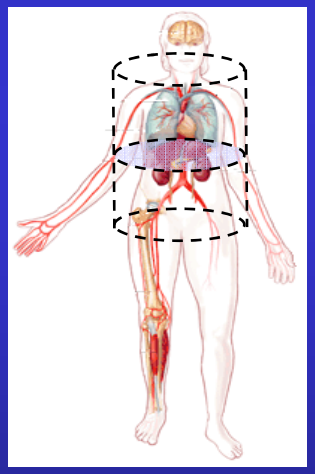

Therapy "A"

Therapy "B"

24 - 48 hours

FDG, FLT

Therapy "A"

X

Therapy "B"

2 months

THE UNIVERSITY OF TEXAS MD ANDERSON CANCER CENTER

Making Cancer History™

Mechanisms of selectivity of EGFR kinase imaging agent

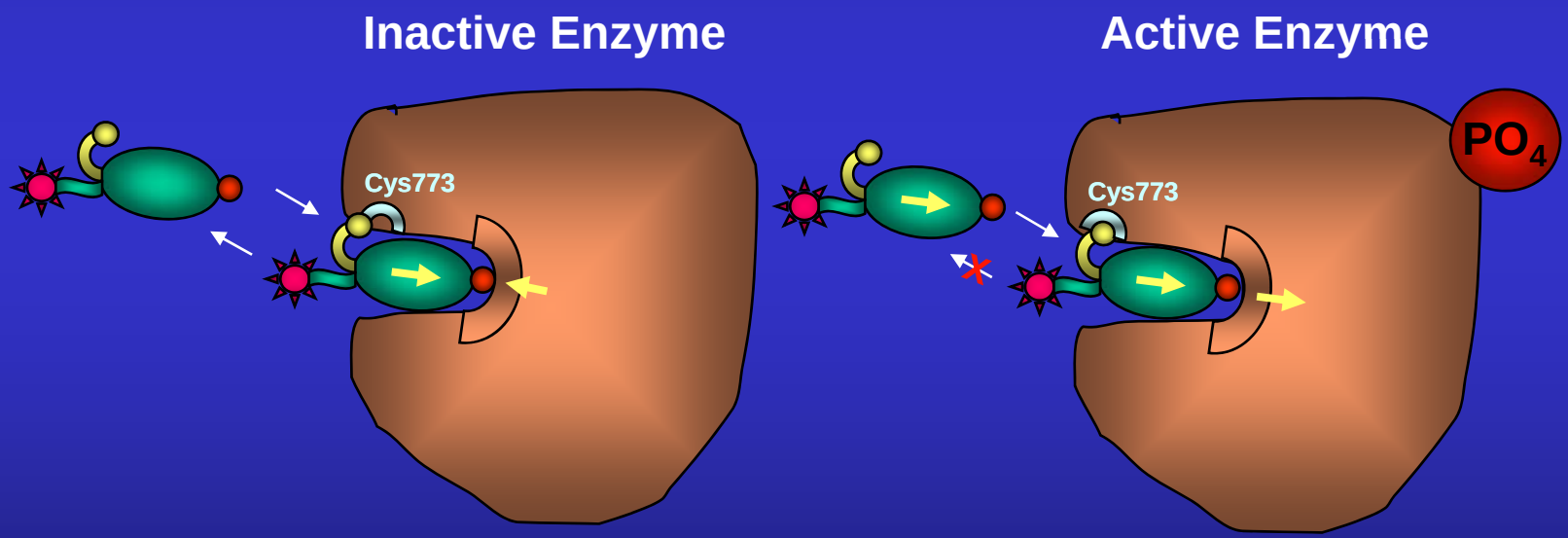

THE UNIVERSITY OF TEXAS
MD ANDERSON
CANCER CENTER
Making Cancer History™

Molecular Imaging Agent for Imaging EGFR kinase expression/activity

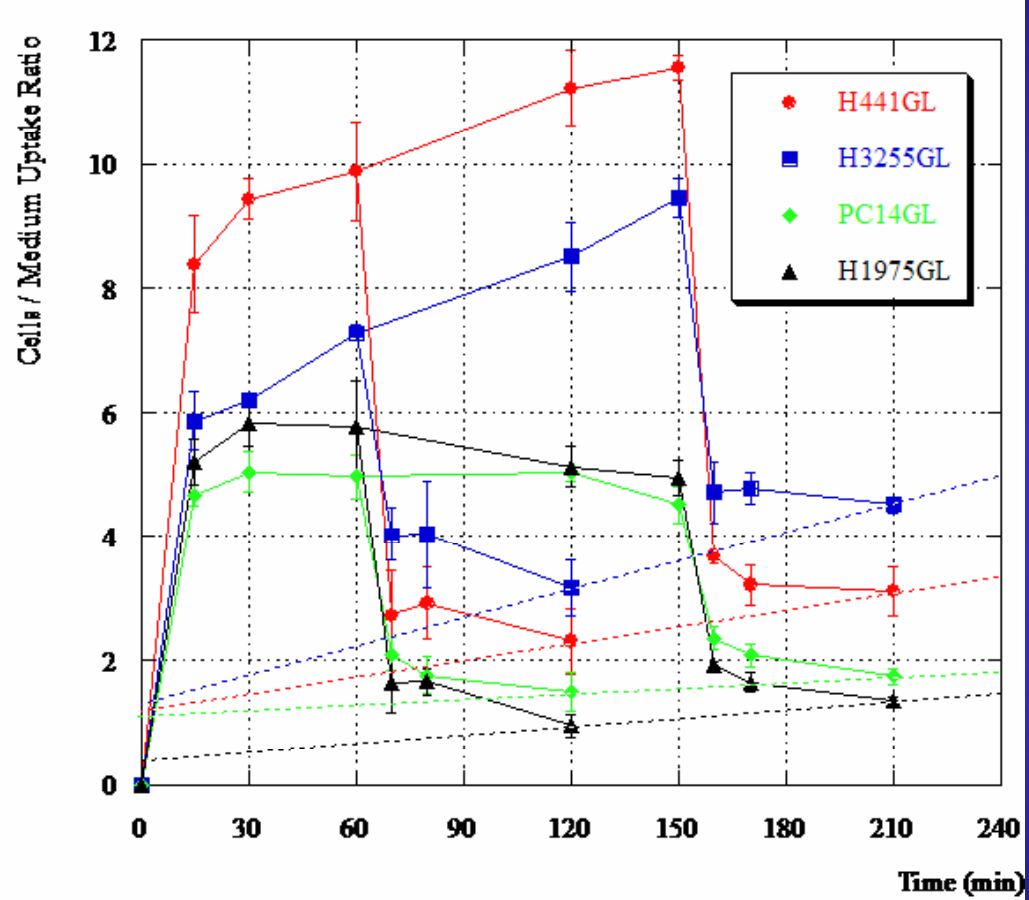

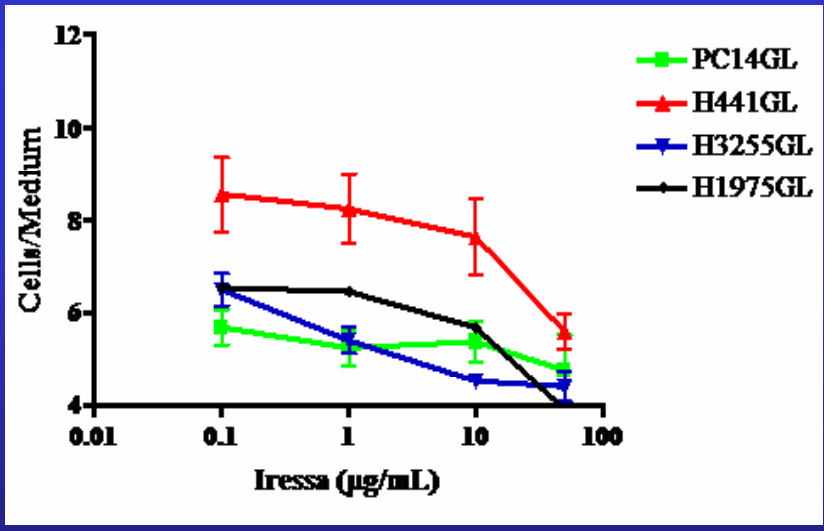

THE UNIVERSITY OF TEXAS MD ANDERSON CANCER CENTER
Making Cancer History™

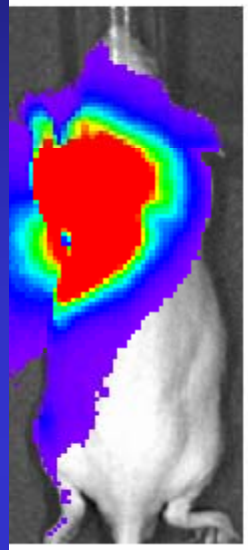

BLI

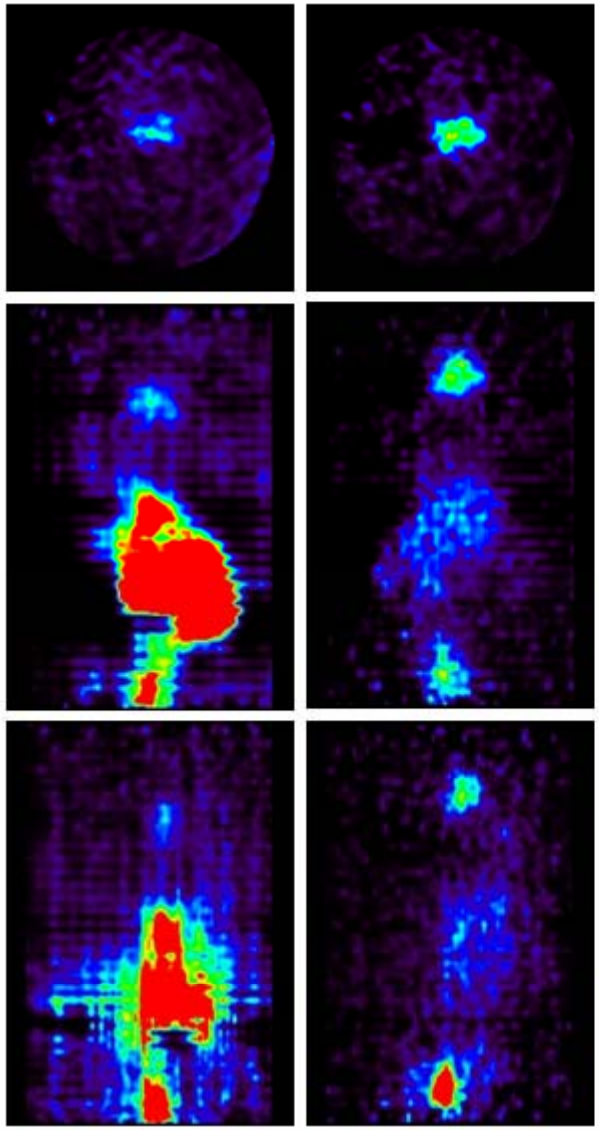

3hr **PET** 24hr

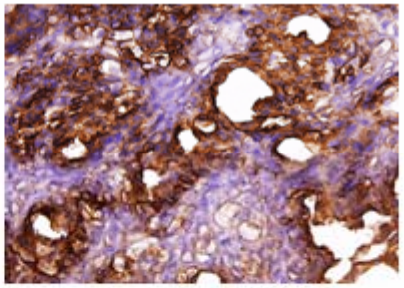

phospho-EGFR expression

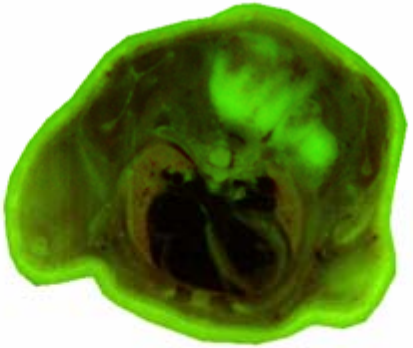

GFP / visible fusion

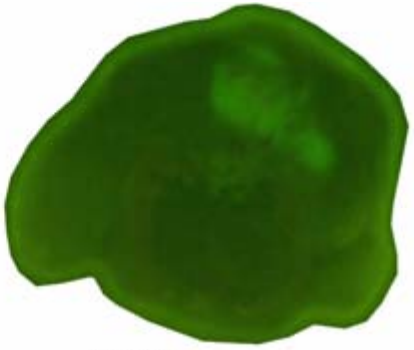

GFP fluorescence

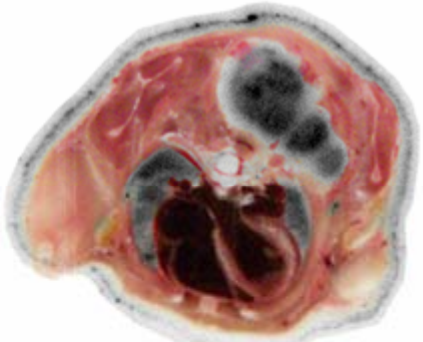

Autoradiography / visible fusion

Visible

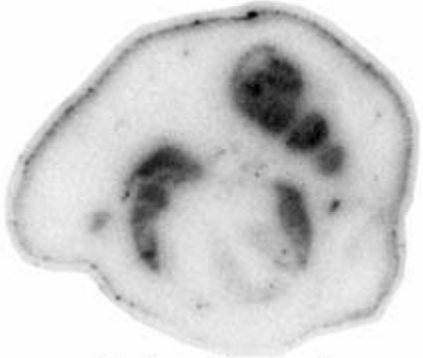

Autoradiography

THE UNIVERSITY OF TEXAS MD ANDERSON CANCER CENTER
Making Cancer History™

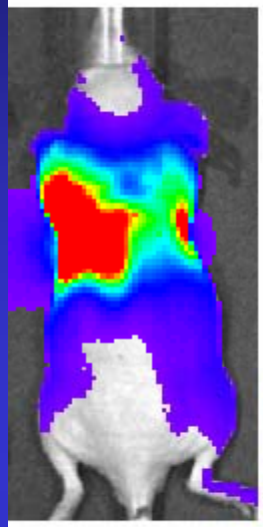

BLI

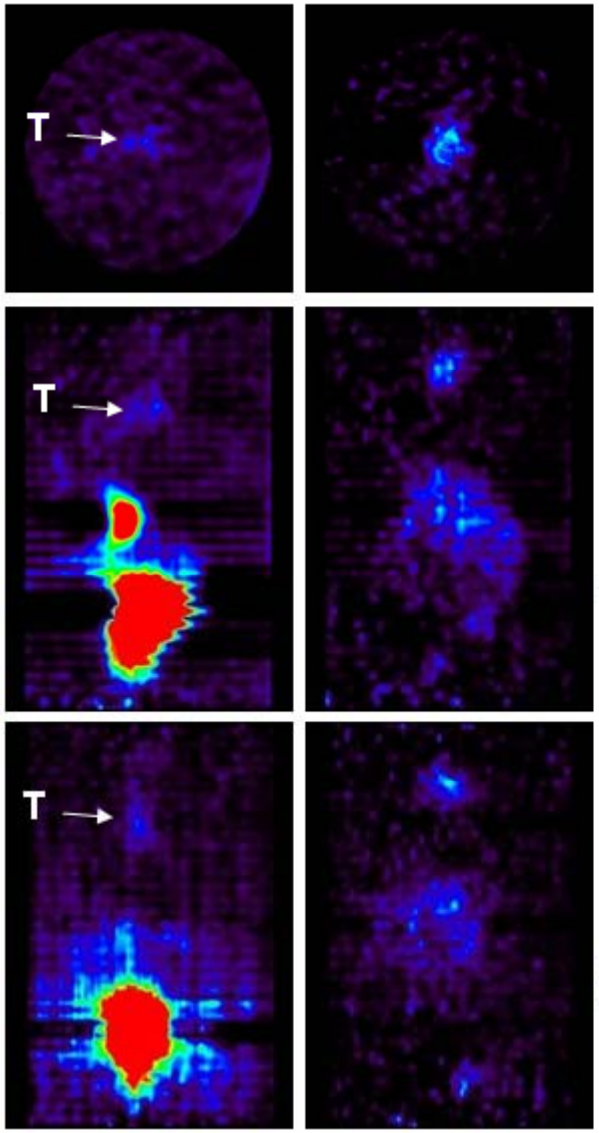

3hr **PET** 24hr

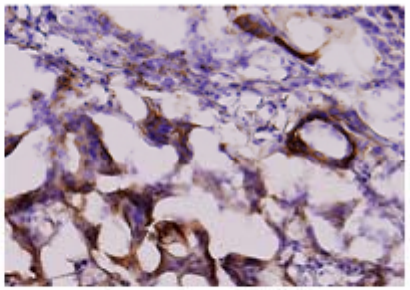

phospho-EGFR expression

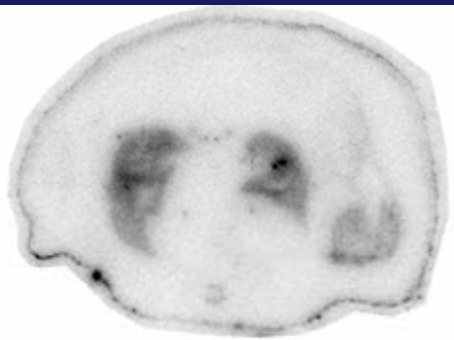

Autoradiography / visible fusion

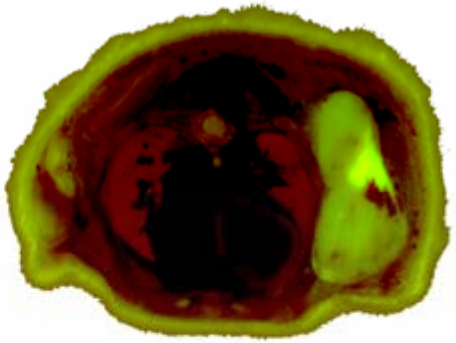

GFP / visible fusion

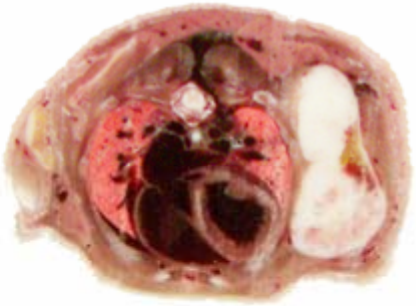

Visible

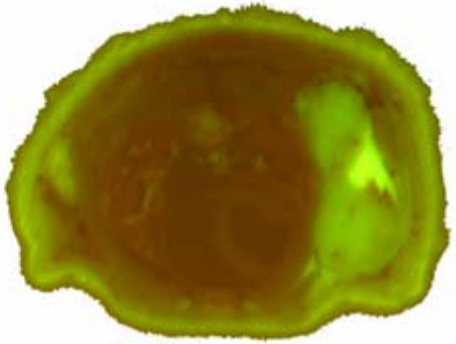

GFP fluorescence

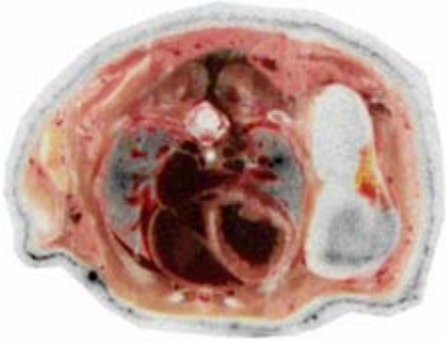

Autoradiography

THE UNIVERSITY OF TEXAS
MD ANDERSON
CANCER CENTER
Making Cancer History™

Non-invasive molecular imaging of EGFR expression-activity with ^{124}I-mIPQA PET/CT in orthotopic U87 glioma xenografts in mice

uPET/uCT

uPET

uCT

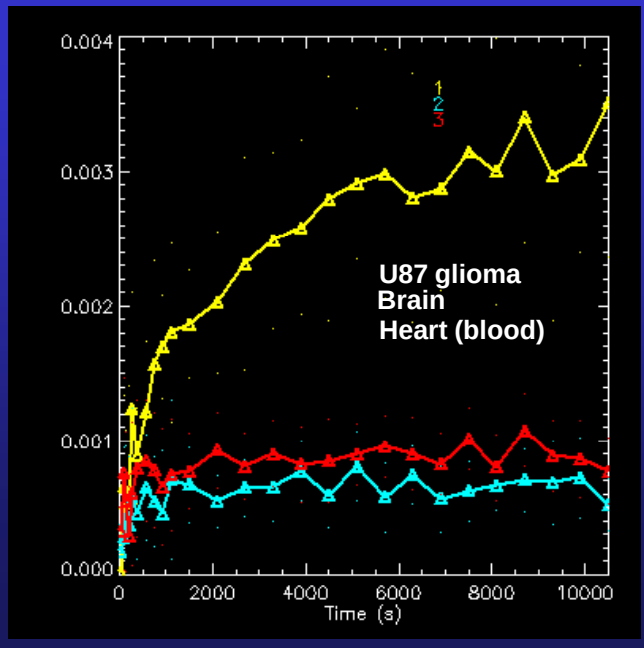

THE UNIVERSITY OF TEXAS
MD ANDERSON
CANCER CENTER
Making Cancer History™

Non-invasive molecular imaging of EGFR expression-activity with ^{124}I-mIPQA PET/CT in intracerebral U87 glioma xenografts in mice

Wild-type EGFR

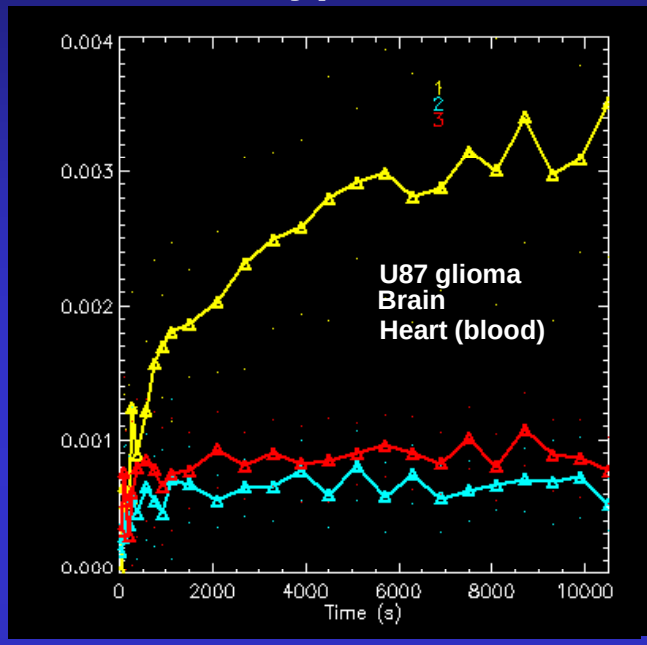

+ EGFRvIII mutant

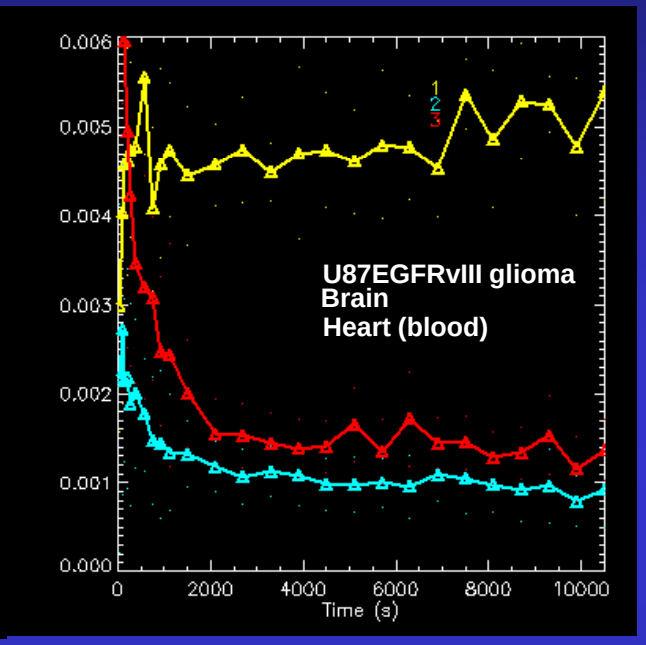

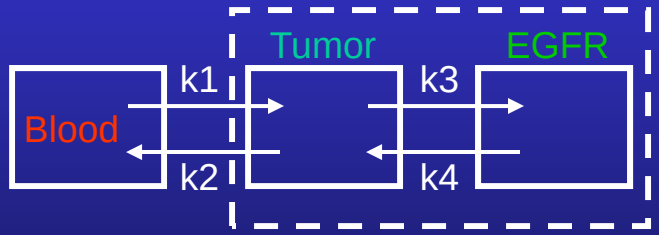

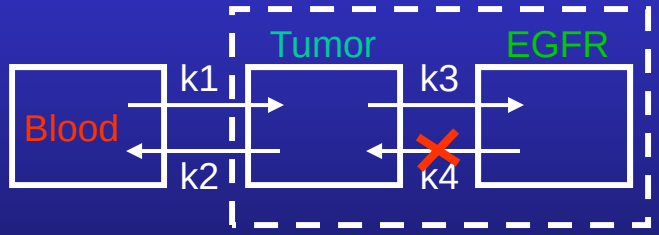

THE UNIVERSITY OF TEXAS
MD ANDERSON
CANCER CENTER
Making Cancer History™

NSCLCs - GL with Iressa

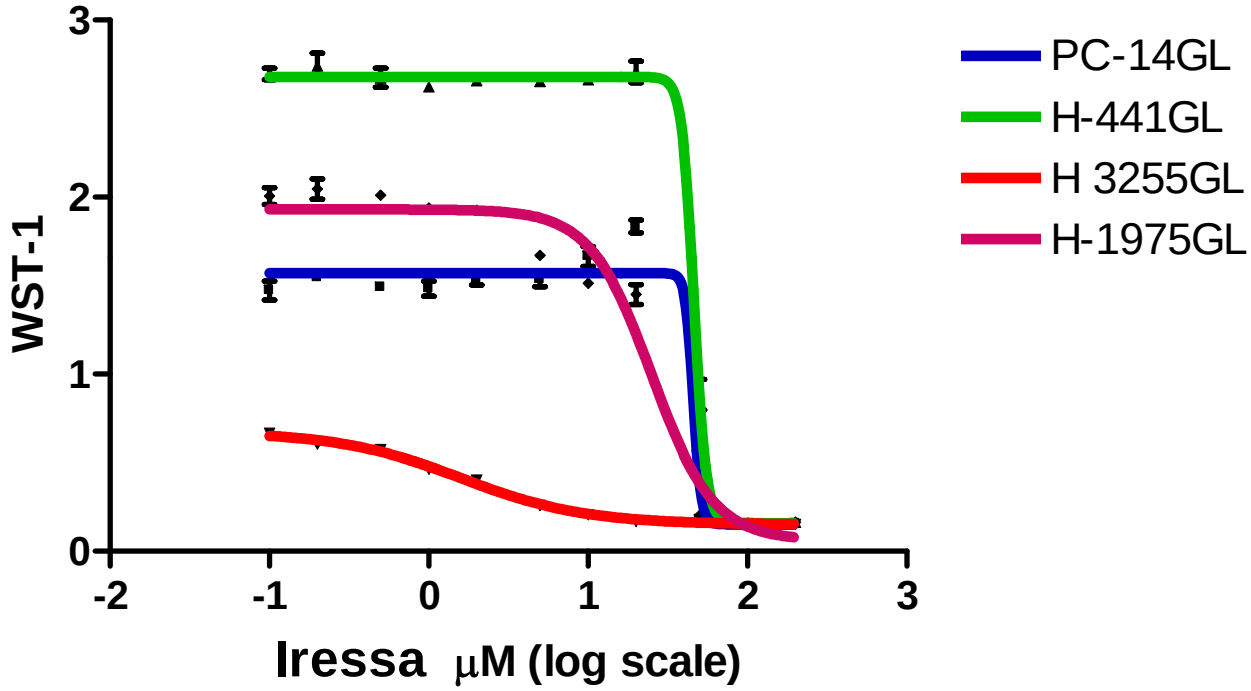

	PC-14GL	H-441GL	H 3255GL	H-1975GL
EC50	45.84	46.19	1.598	25.09

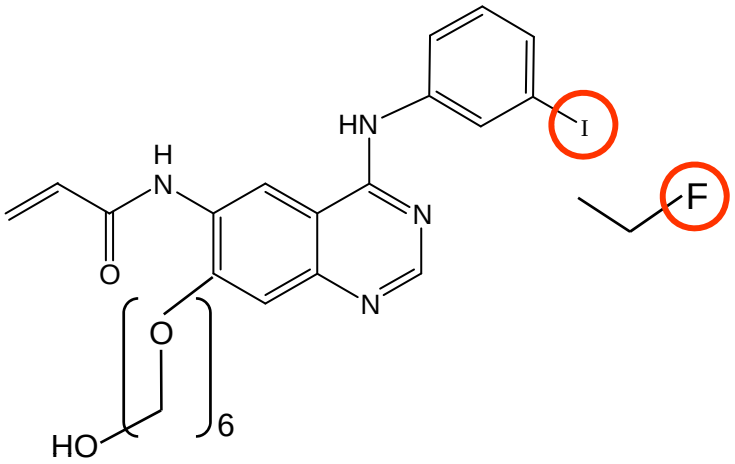
HN
H
N
O
N
N
O
6
HO
I
F

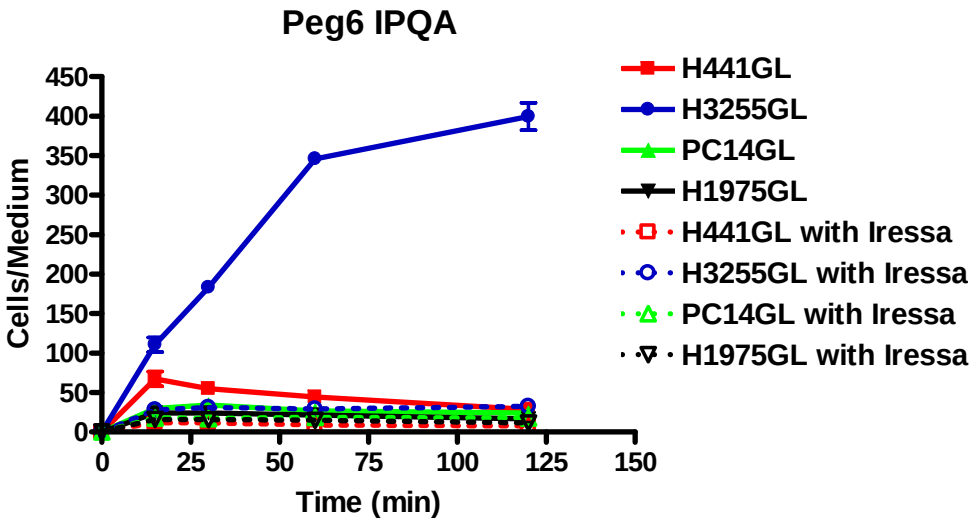
Peg6 IPQA
Cells/Medium
Time (min)
H441GL
H3255GL
PC14GL
H1975GL
H441GL with Iressa
H3255GL with Iressa
PC14GL with Iressa
H1975GL with Iressa

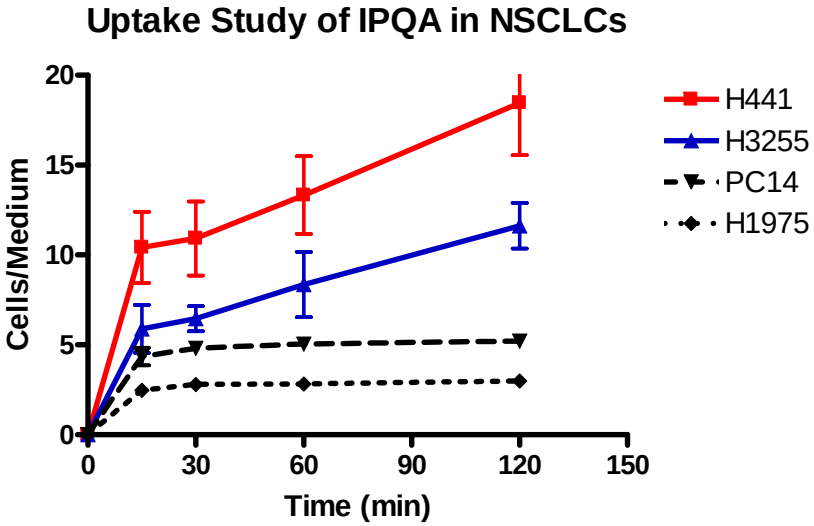
Uptake Study of IPQA in NSCLCs
Cells/Medium
Time (min)
H441
H3255
PC14
H1975

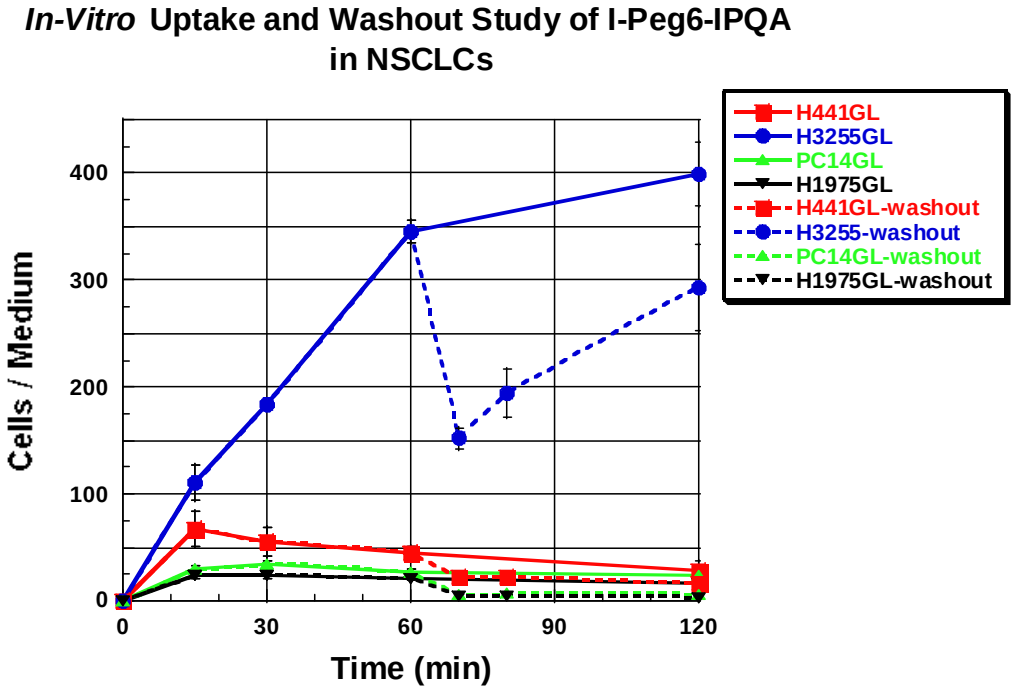
In-Vitro Uptake and Washout Study of I-Peg6-IPQA in NSCLCs
Cells / Medium
Time (min)
H441GL
H3255GL
PC14GL
H1975GL
H441GL-washout
H3255-washout
PC14GL-washout
H1975GL-washout

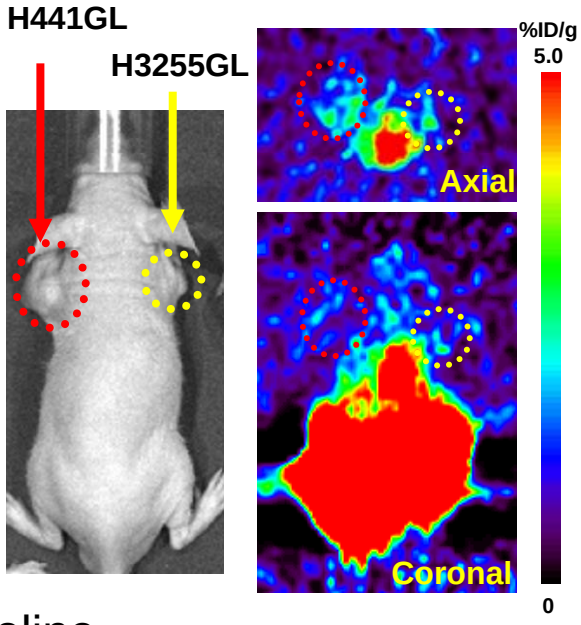

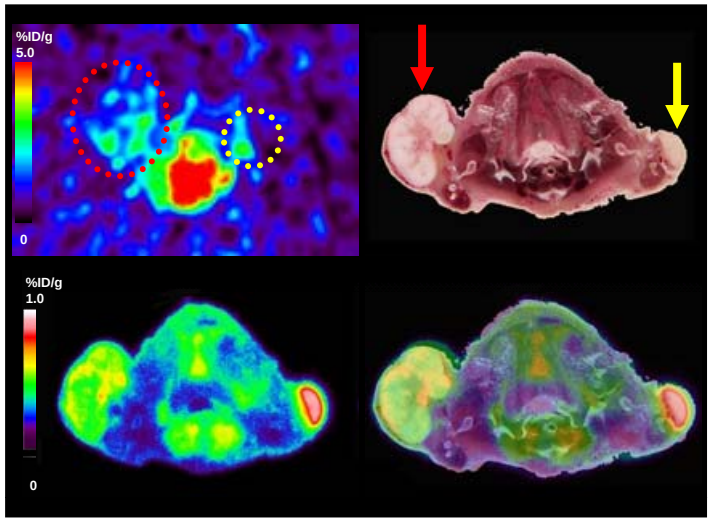

Baseline

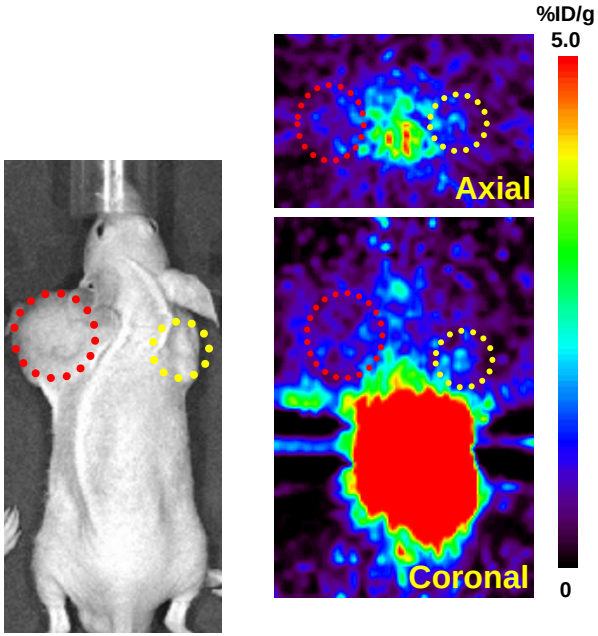

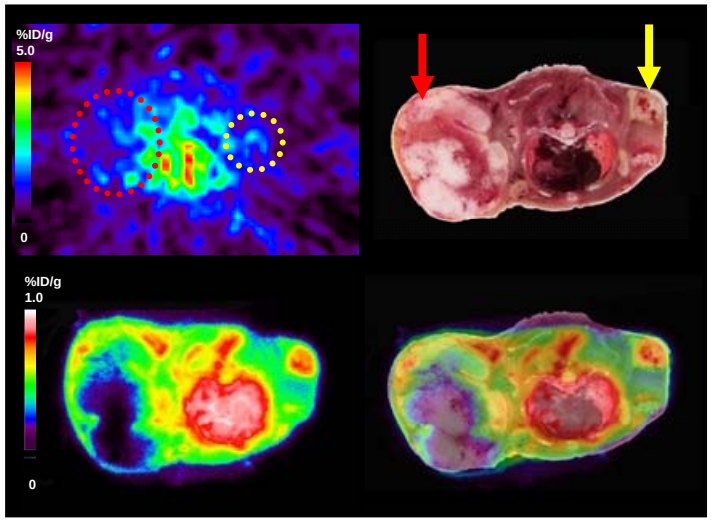

With Inhibitor 3h

Inhibitor: gefitinib, 100mg/kg,i.p.
1h prior to the radiotracer

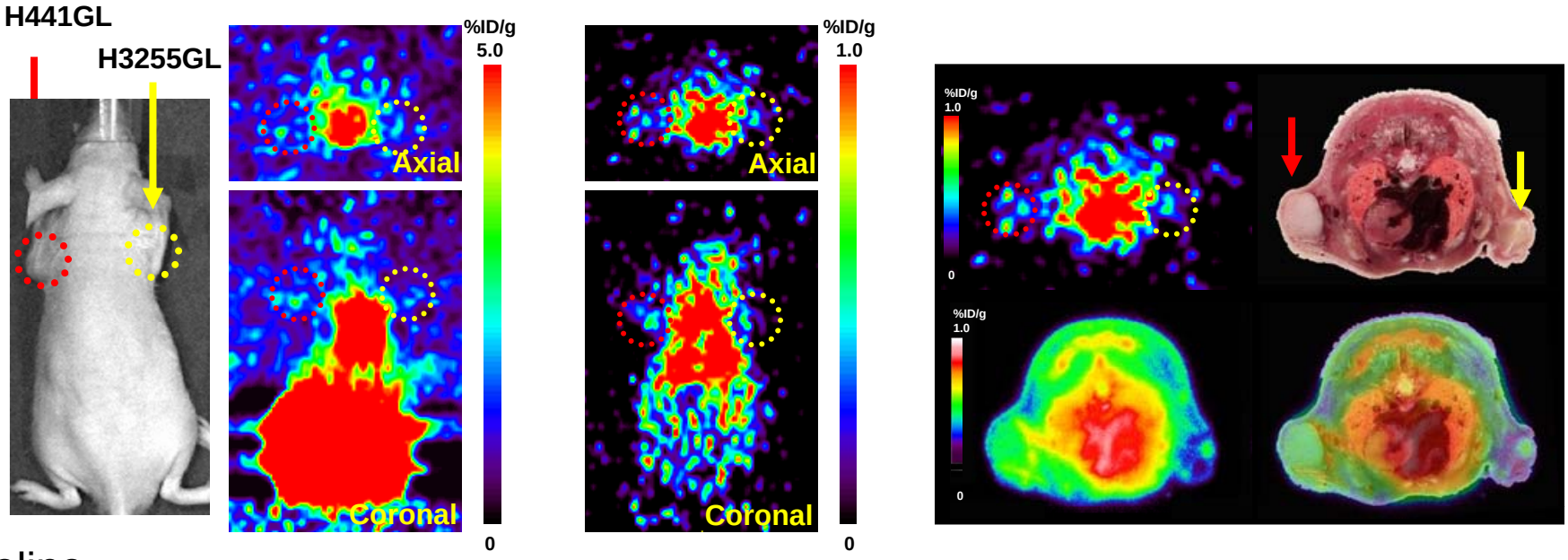

Baseline

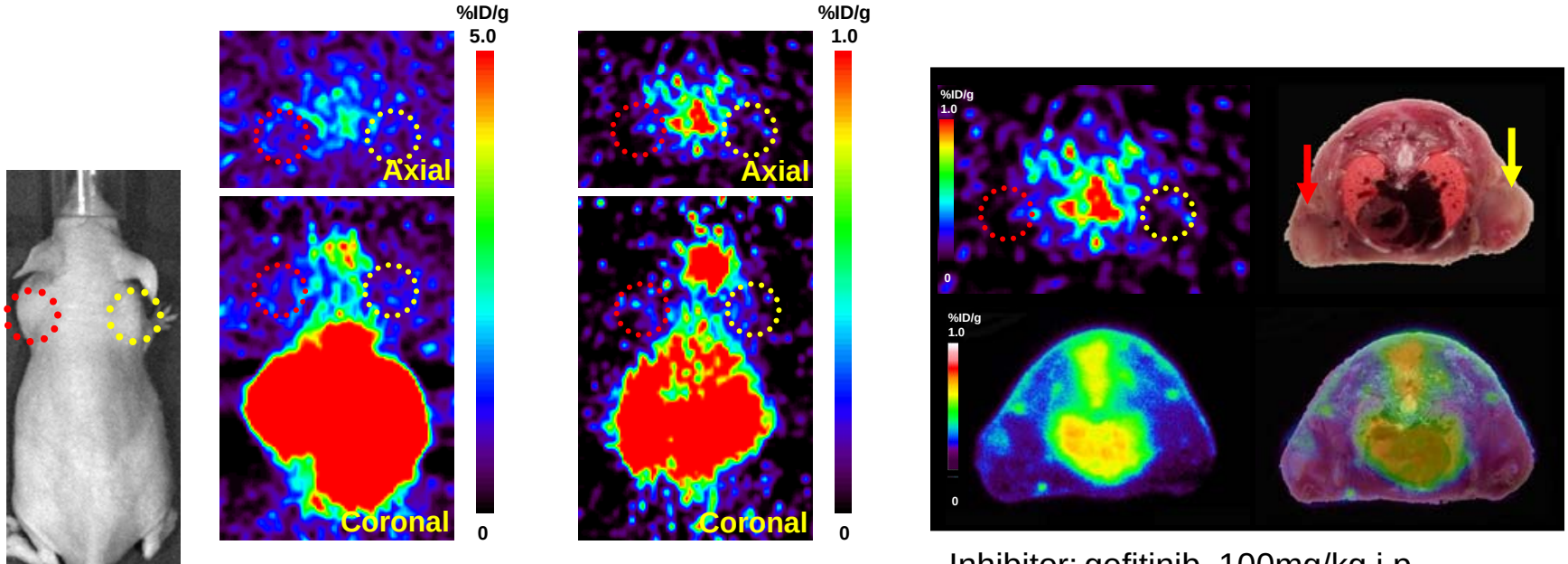

With Inhibitor 3h 24h

Inhibitor: gefitinib, 100mg/kg,i.p.
1h prior to the radiotracer

A Paradigm for Therapy Selection and Monitoring by Imaging (Part II)

PET/CT

FDG
FLT
EGFR
k-Ras mutant

EGFR mutant
FDG
FLT
EGFR

Chemo-Radiation
k-Ras inhibitor

EGFR Inhibitor

After 1 cycle (or @ 24-72h)

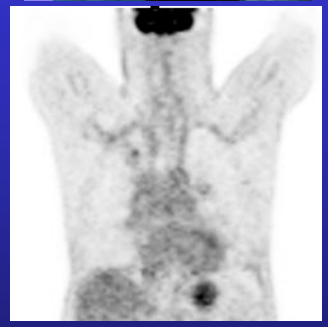

FDG
FLT
EGFR

Chemo-Radiation
k-Ras inhibitor

FDG
FLT
EGFR

EGFR Inhibitor

Key Imaging Targets:
EGFR, DNA synth.

THE UNIVERSITY OF TEXAS MD ANDERSON CANCER CENTER
Making Cancer History™

Integration of Molecular Imaging, Interventional Radiology, and Tumor Biomarkers

PET/CT Imaging

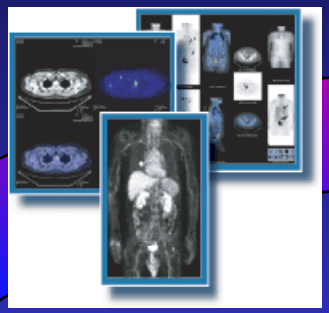

PK/PD Modeling
Parametric Imaging

Parametric Image-Guided
Biopsy (or Intraoperative)

HISTOPATHOLOGY
Immunohistochemistry

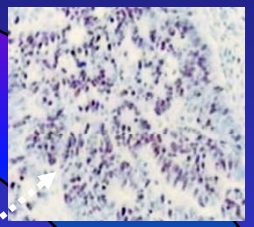

Tumor Lysate
Arrays

microPET/CT Imaging

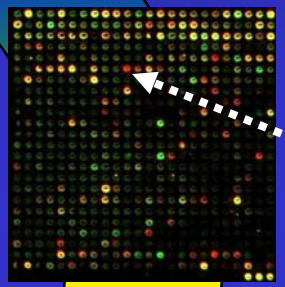

Drug Target

GENOMICS

Radiolabeling

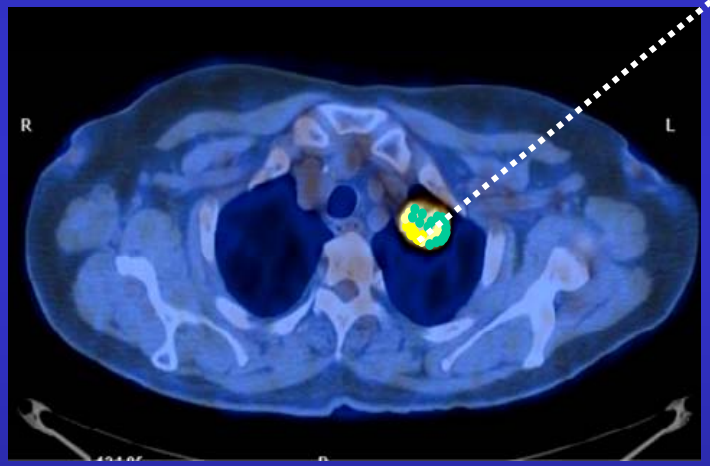

Structural
Biochemistry

In Silico Modeling

Cyclotron
Radionuclid

Radiotracer
Precursors

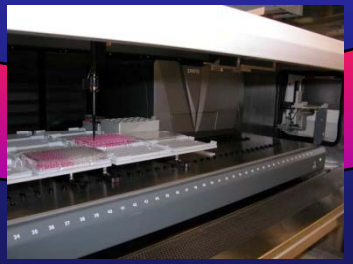

HT/HC Screning

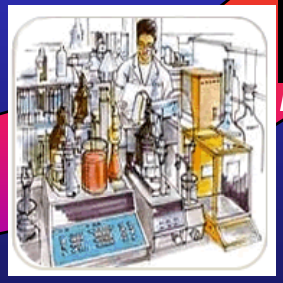

New Chemistry

THE UNIVERSITY OF TEXAS
MD ANDERSON
CANCER CENTER
Making Cancer History™